Self-interacting dark matter: non-perturbative dynamics

Ayuki Kamada (University of Warsaw)

Based on
<u>AK</u>, Takumi Kuwahara and Ami Patel, JHEP, 2023
<u>AK</u> and Takumi Kuwahara, in progress

Sep. 17, 2026 @ Particle Physics in the Early Universe

Dark matter

DM (or missing mass)

- evident from cosmological observations

    - cosmic microwave background (CMB)…

- essential to form galaxies in the Universe

- one of the biggest mysteries

    - astronomy, cosmology, particle physics…

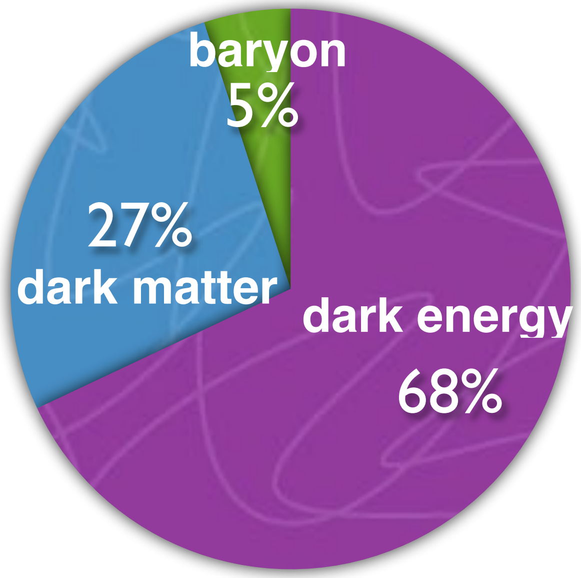

cosmic energy budget

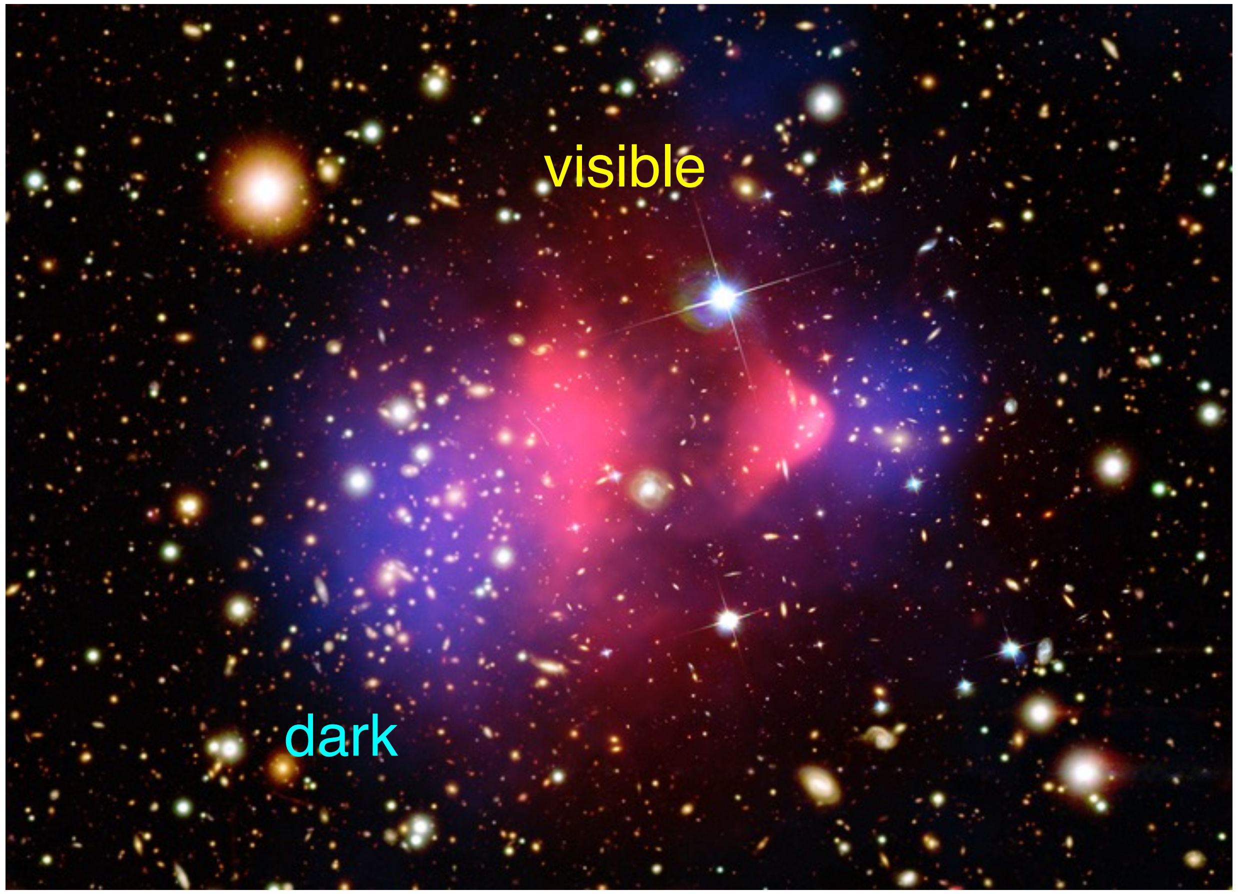

bullet cluster

(Old but) new approach

Gravitational probes

- complementary to direct, indirect and collider searches
- how visible matter distribution changes w/ DM properties
- all known properties are derived in this way (including its existence; standard model (SM) neutrinos are too hot to form galaxies)

Self-interacting dark matter (SIDM)

- interactions among dark matter particles
    - hard to probe in other searches

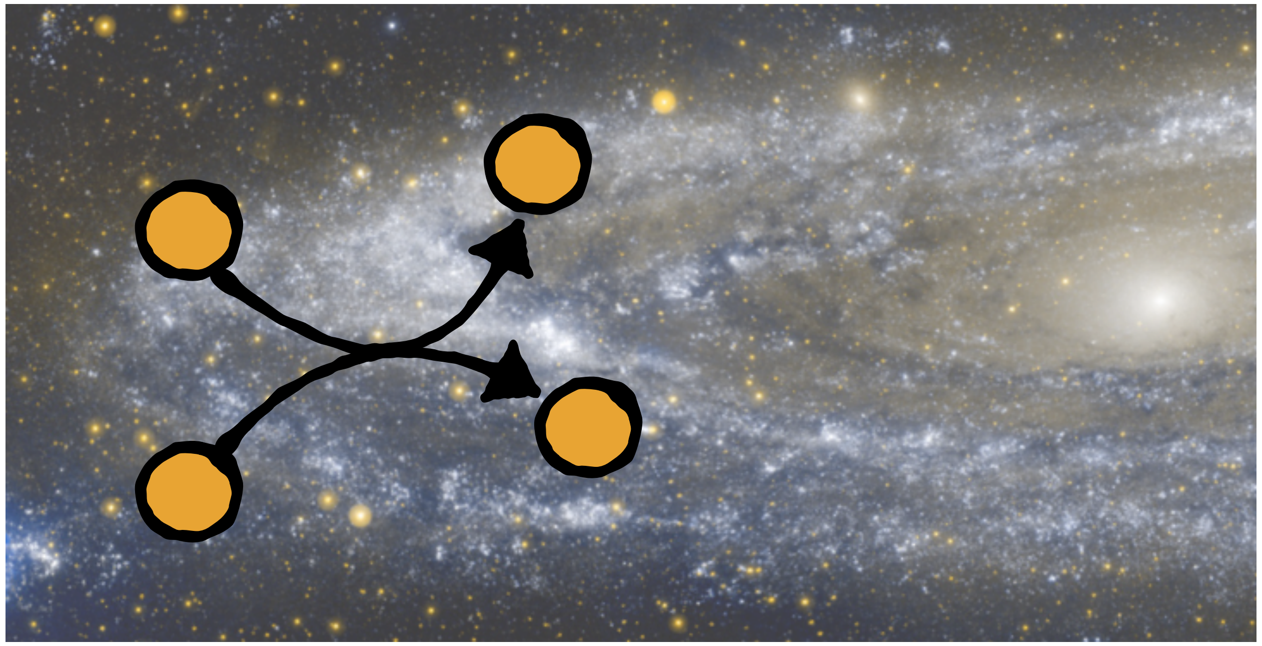

Contents

Self-interacting dark matter

Self-interacting dark matter (SIDM)

- dark matter density profile inside a halo turns from cuspy to cored

  - cored profile “appear to” provide better fit to astronomical data

  - though, stellar feedback should be taken into account

$$\sigma/m \sim 1\,\mathrm{cm}^2/\mathrm{g} \sim 1\,\mathrm{barn}/\mathrm{GeV}$$

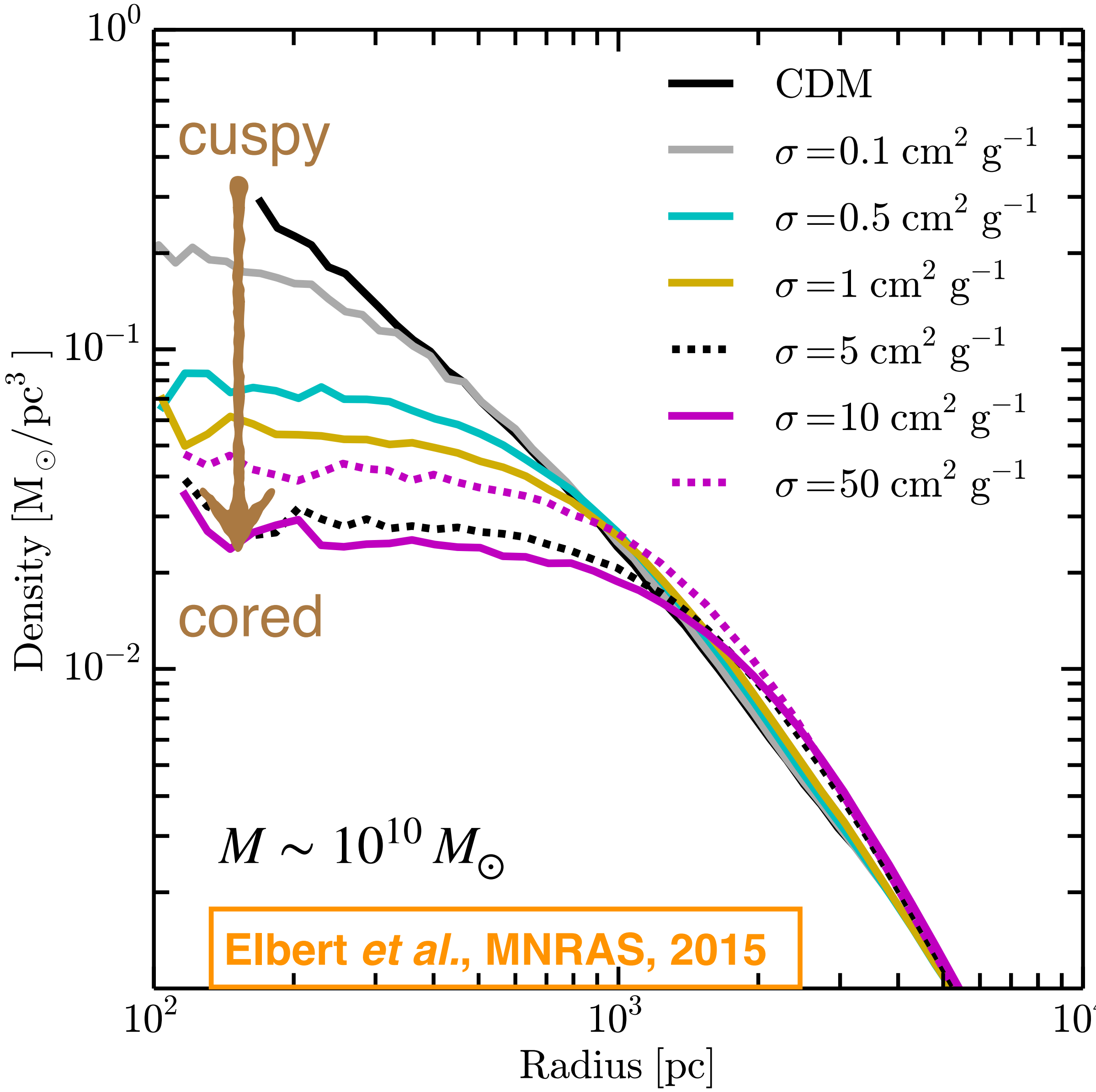

1st stage of SIDM

Core vs cusp problem (1994)

- dwarf galaxies appear to prefer a cored profile

SIDM as an explanation (1999)

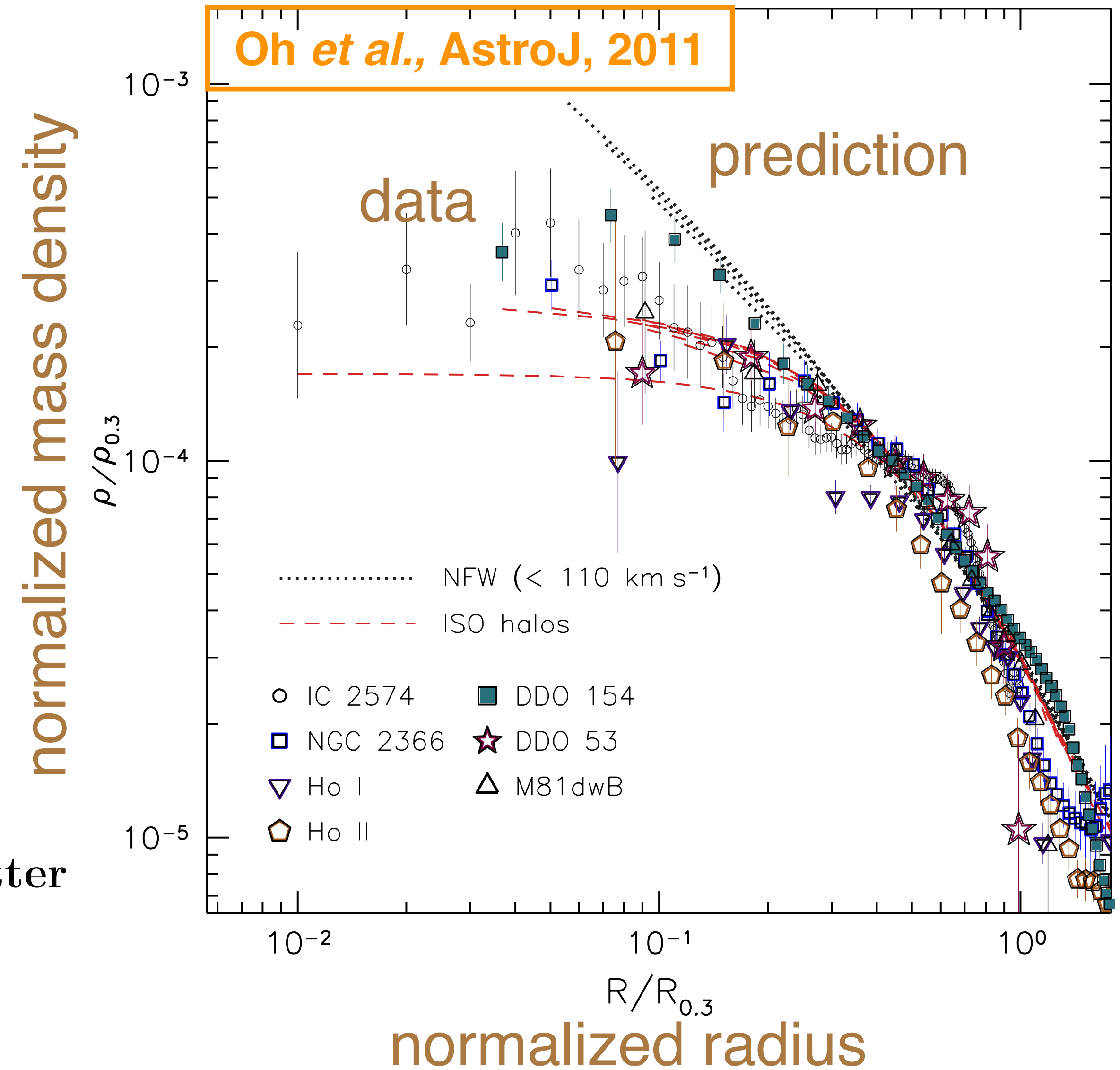

Observational evidence for self-interacting cold dark matter

David N. Spergel and Paul J. Steinhardt
Princeton University, Princeton NJ 08544 USA

Cosmological models with cold dark matter composed of weakly interacting particles predict overly dense cores in the centers of galaxies and clusters and an overly large number of halos within the Local Group compared to actual observations. We propose that the conflict can be resolved if the cold dark matter particles are self-interacting with a large scattering cross-section but negligible annihilation or dissipation. In this scenario, astronomical observations may enable us to study dark matter properties that are inaccessible in the laboratory.

To summarize, our estimated range of σ/m for the dark matter is between 0.45-450 cm^2/g or, equivalently, $8 \times 10^{-(25-22)}$ cm^2/GeV. Numerical calculations are es-

2nd stage of SIDM

Overview

- cores in various-size halos may prefer velocity dependence of self-scattering cross section

- dwarf spiral galaxy (IC 2574)

$M \sim 10^{11} M_\odot$

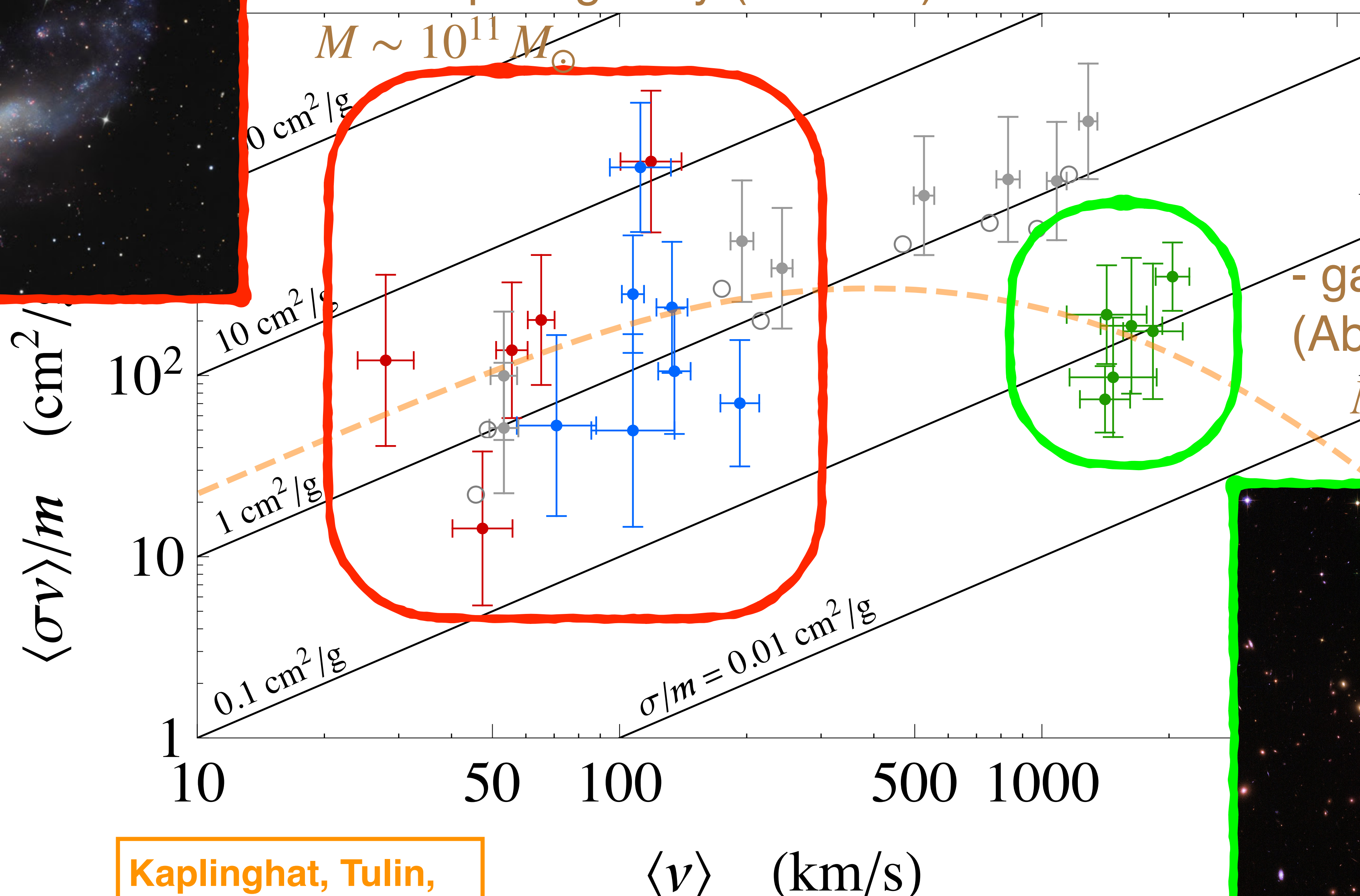

- galaxy cluster (Abell 2744)

$M \sim 10^{14} M_\odot$

Kaplinghat, Tulin, and Yu, PRL, 2016

“Data” points

Light mediator fit to data

- DM and mediator masses are pinned down $m_\chi \sim 10\,\mathrm{GeV}$ $\;m_\phi \sim 10\,\mathrm{MeV}$

  - repulsive Yukawa (for simplicity)

$\alpha_\chi = \alpha_{\mathrm{em}}$

$$V = \frac{\alpha_\chi}{r} e^{-m_\phi r}$$

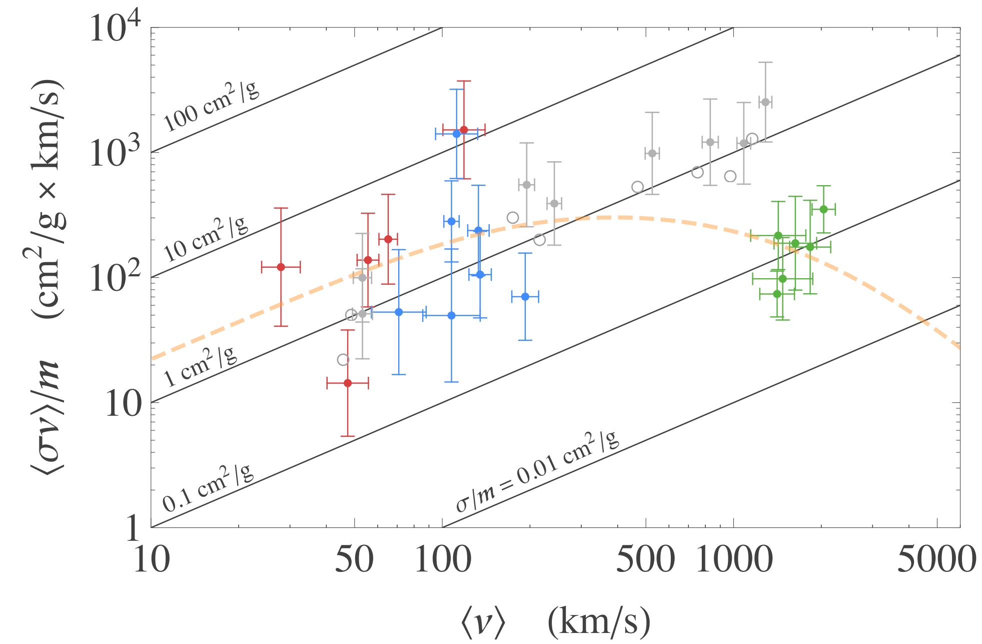

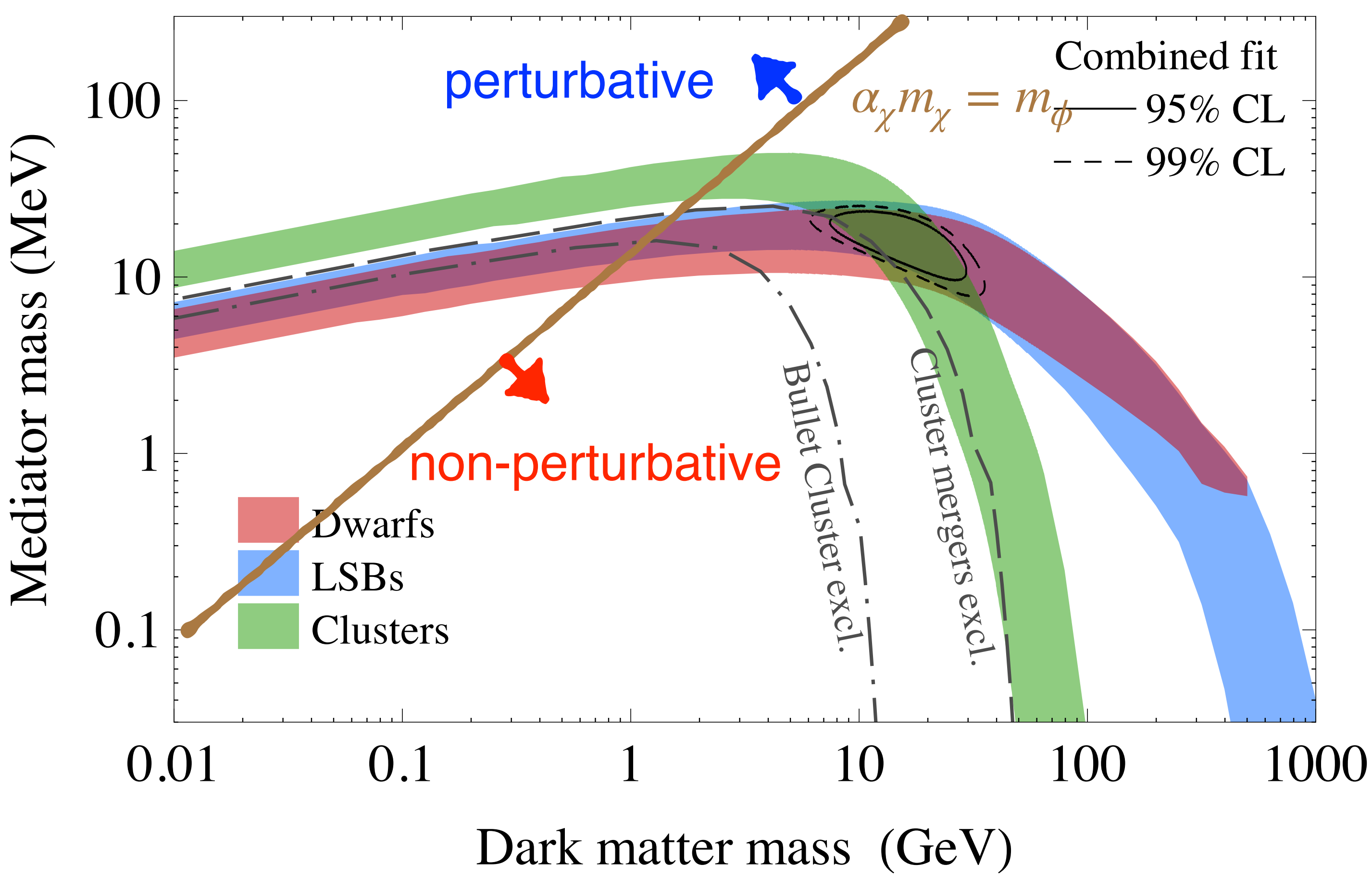

- perturbative: Born (tree-level) approximation is good

- non-perturbative: need to solve Schrödinger equation (resummation of ladder diagrams)

Tulin, Yu, and Zurek, PRD, 2013

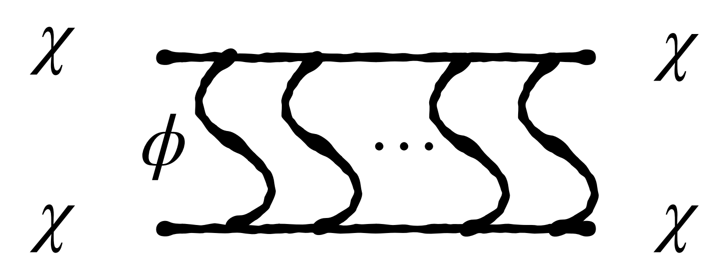

Contents

Self-interacting dark matter

- core formation in halos

How to find SIDM cross section

- beyond-Born approximation (perturbation)

Dissipative SIDM

- gravothermal collapse

How to find bremsstrahlung cross section

- distorted-wave Born approximation

Scattering in quantum mechanics

Schrödinger equation

Weinberg, "Lectures on Quantum Mechanics"

$$\left[-\frac{1}{2\mu}\nabla^2 + V(r)\right]\psi_p(\vec{r}) = E\psi_p(\vec{r}) \qquad E = \frac{p^2}{2\mu} \qquad p = \mu v_{\rm rel}$$

- reduced mass ($\mu = m/2$ for same-mass particles)

- potential from long-range force

- scattering state (energy-eigenstate of Schrödinger equation)

$$\psi_p(\vec{r}) \to e^{ipz} + f(p,\theta)\frac{e^{ipr}}{r} \qquad r \to \infty$$

- (initial) plane wave

- scattering amplitude

- out-going spherical wave

Born approximation

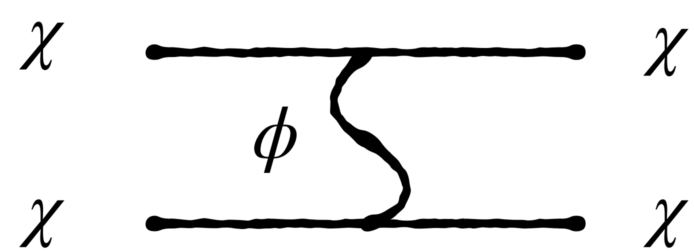

- Lippmann–Schwinger equation

$$\psi_p(\vec{r}) = e^{ipz} + \int d^3x' G(\vec{r} - \vec{r}')V(r')\psi_p(\vec{x}') \qquad G(\vec{r}) = -\frac{2\mu}{4\pi r}e^{ipr}$$

- leading order

$$f(p,\theta) = -\frac{\mu}{2\pi}\int d^3x V(r) e^{i\vec{q}\cdot\vec{x}}$$

- Fourier transformation $\quad \vec{q} = \vec{p} - \vec{p}'$

Scattering in quantum mechanics

Partial-wave decomposition

- motivated by $e^{ipz} = \sum_{\ell=0}^{\infty} (2\ell+1) i^{\ell} j_{\ell}(pr) P_{\ell}(\cos\theta)$

$$\psi_p(\vec{r}) = \sum_{\ell=0}^{\infty} (2\ell+1) i^{\ell} \frac{1}{p} R_{p,\ell}(r) P_{\ell}(\cos\theta)$$

Scattering phase shift

- radial wave function at the origin (regularity)

$$R_{p,\ell}(r) \to \mathcal{O}(r^{\ell}) \quad r \to 0$$

- radial wave function at infinity

$$R_{p,\ell}(r) \to \frac{i}{2r}\left[e^{-i(pr-\frac{1}{2}\ell\pi)} - e^{2i\delta_\ell} e^{i(pr-\frac{1}{2}\ell\pi)}\right] \quad r \to \infty$$

$$f(p,\theta) = \sum_{\ell=0}^{\infty} (2\ell+1) f_{\ell}(p) P_{\ell}(\cos\theta) \quad f_{\ell}(p) = \frac{e^{2i\delta_\ell(p)} - 1}{2ip}$$

$$\sigma = \sum_{\ell=0}^{\infty} \sigma_\ell \qquad \sigma_\ell = \frac{4\pi}{p^2}(2\ell+1)\sin^2\delta_\ell(p)$$

- diagonalized S-matrix

$$S_\ell(p) = e^{2i\delta_\ell(p)}$$

Jost function

How to find $R_{k,\ell}(r)$ in practice?

AK, Kuwahara and Patel, JHEP, 2023

AK, Matsumoto and Patel and Watanabe, in progress

- "initial" condition given at the origin (regularity)

$$\mathscr{R}_{p,\ell}(r) \to p j_\ell(pr) \approx p \frac{(pr)^\ell}{(2\ell+1)!!} \quad r \to 0$$

- radial Schrödinger equation

$$\left[\frac{1}{r^2}\frac{d}{dr}r^2\frac{d}{dr} + p^2 - \frac{\ell(\ell+1)}{r^2} - 2\mu V(r)\right]\mathscr{R}_{p,\ell}(r) = 0$$

- asymptotic behavior of solution

$$\mathscr{R}_{p,\ell}(r) \to \frac{i}{2r}\left[\mathscr{J}_\ell(p)e^{-i\left(pr-\frac{1}{2}\ell\pi\right)} - \mathscr{J}_\ell(-p)e^{i\left(pr-\frac{1}{2}\ell\pi\right)}\right] \quad r \to \infty$$

- Jost function

- by comparing asymptotic behavior

$$R_{p,\ell}(r) = \frac{1}{|\mathscr{J}_\ell(p)|}\mathscr{R}_{p,\ell}(r) \quad S_\ell(p) = e^{2i\delta_\ell(p)} = \frac{\mathscr{J}_\ell(-p)}{\mathscr{J}_\ell(p)}$$

- Sommerfeld enhancement factor

$$S_\ell(k) = \frac{1}{|\mathscr{J}_\ell(k)|^2}$$

Three regimes

Tulin, Yu and Zurek, PRD, 2013

Born regime

- well approximated by Born approximation

Resonant (quantum) regime

- well approximated by a couple of lowest-order partial waves
- zero-energy resonances (shallow bound states)

Classical regime

- higher partial waves are required
- fitting formula is known

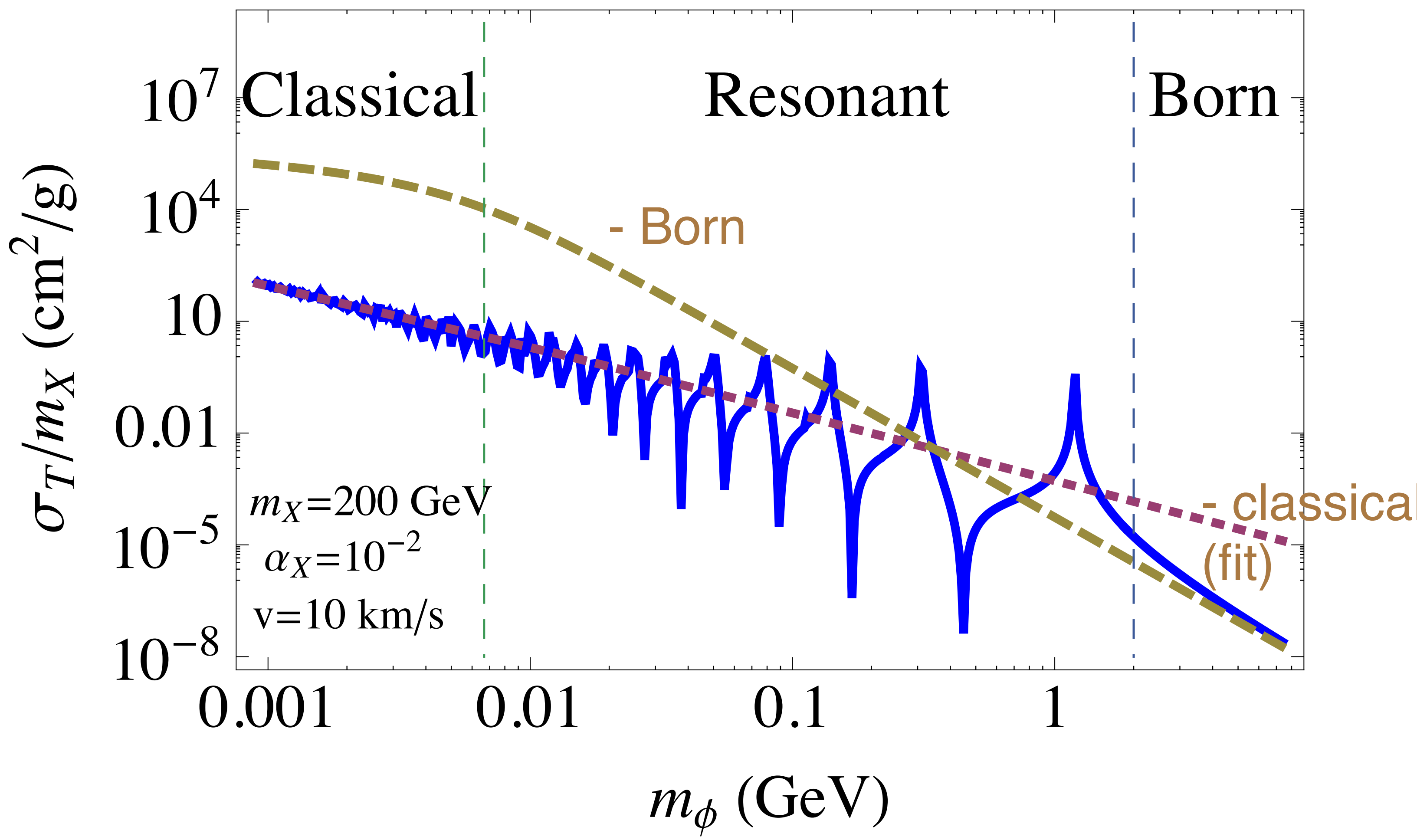

Contents

Self-interacting dark matter

- core formation in halos

How to find SIDM cross section

- beyond-Born approximation (perturbation)

Dissipative SIDM

- gravothermal collapse

How to find bremsstrahlung cross section

- distorted-wave Born approximation

Gravothermal collapse

SIDM

- core formation → core collapse

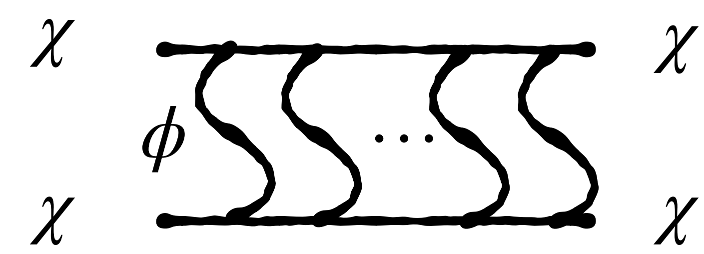

Dissipation (cooling)

- accelerates core collapse

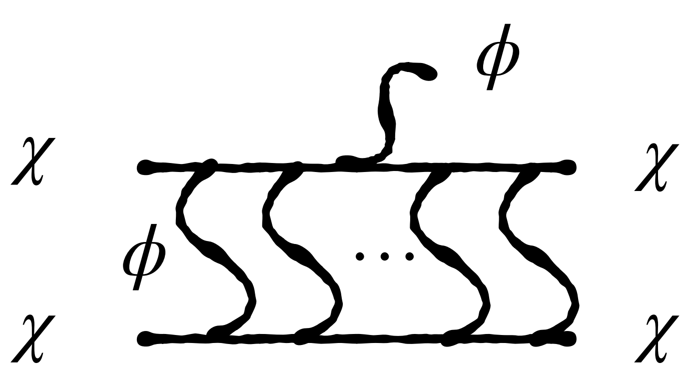

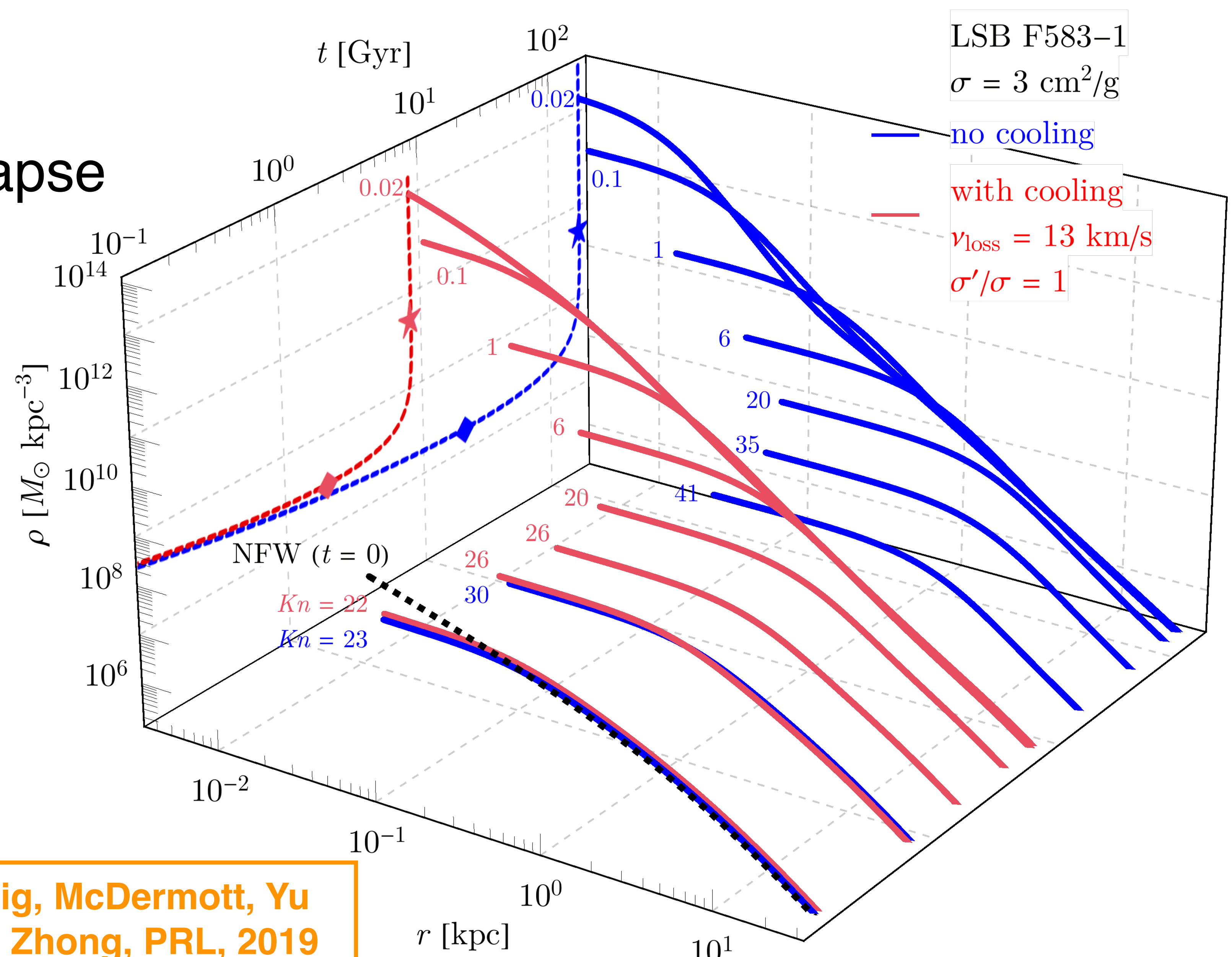

Essig, McDermott, Yu and Zhong, PRL, 2019

Diversity in MW satellites

MW satellites (classical)

- mass distribution is determined by line-of-sight velocity dispersion (LOSVD) profile

- shows diversity in inner slope and density, though uncertainty is still large

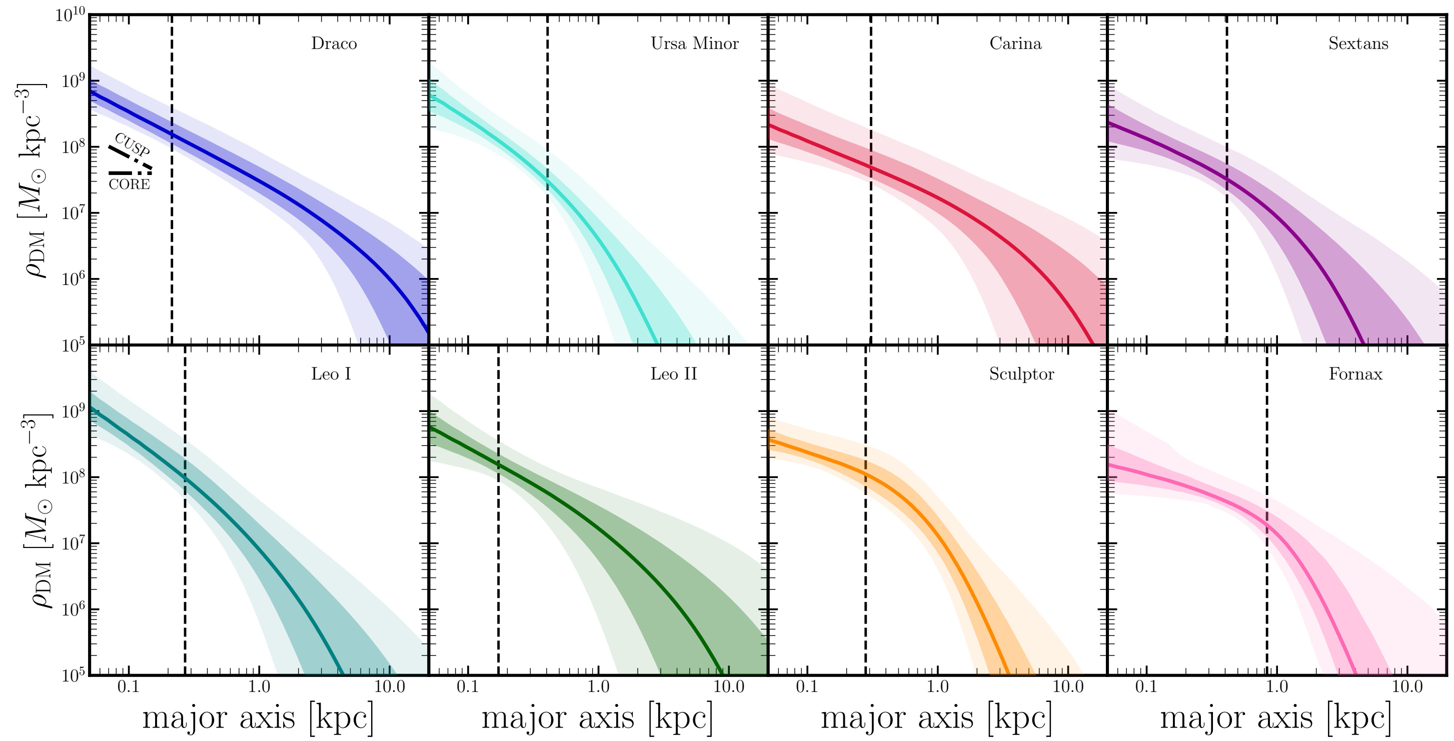

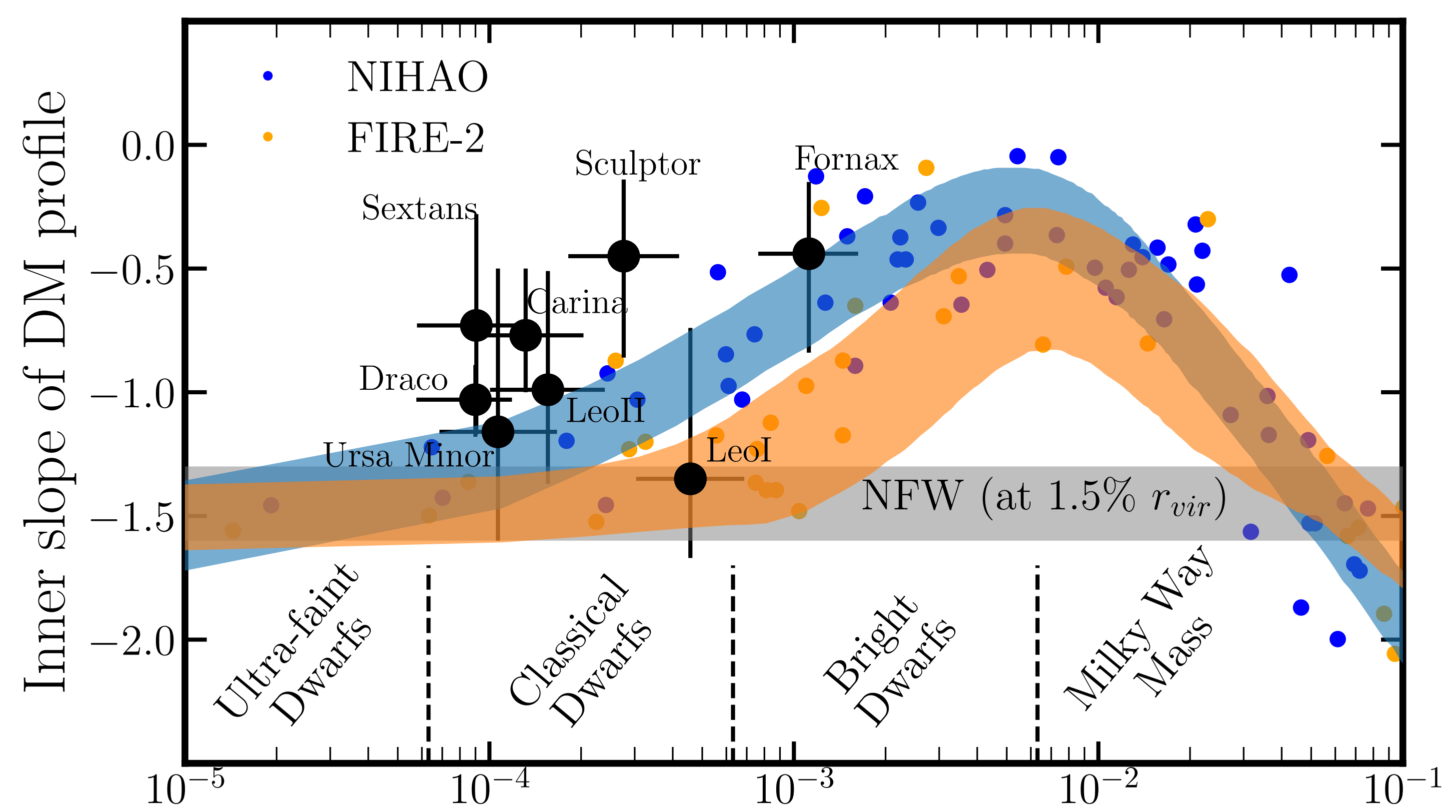

Hayashi, Chiba, and Ishiyama, ApJ, 2020

Strong SIDM

Gravothermal collapse

- tidal stripping: different orbits in MW → different "initial" profiles
- stripped profile sees accelerated gravothermal collapse

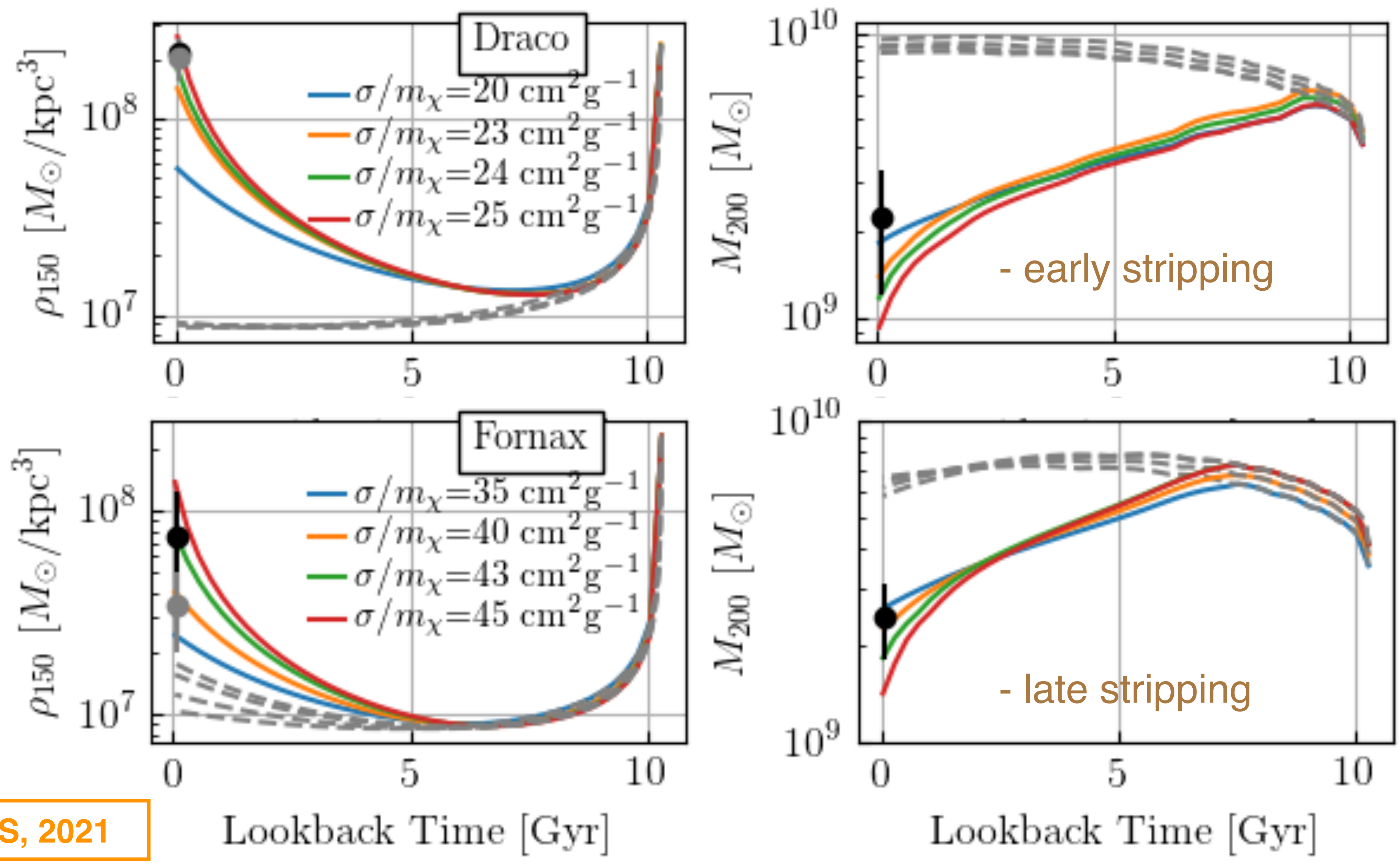

Correa, MNRAS, 2021

Collapsed objects

Perturber of strong lens system

A possible challenge for cold and warm dark matter

Received: 16 September 2025

Accepted: 13 November 2025

Published online: 05 January 2026

Check for updates

Simona Vegetti[1], Simon D. M. White[1], John P. McKean[2,3,4], Devon M. Powell[1], Cristiana Spingola[5], Davide Massari[6], Giulia Despali[6,7,8] & Christopher D. Fassnacht[9]

Measuring the density profile and mass concentration of dark-matter haloes is a key test of the standard cold dark matter paradigm. Such objects are dark and thus challenging to characterize, but they can be studied via gravitational lensing. Recently, a million-solar-mass object was discovered superposed on an extended and extremely thin gravitational arc. Here we report on extensive tests of various assumptions for the mass density profile and redshift of this object. We find that models that best describe the data have two components: an unresolved point mass of radius ≤10 pc centred on an extended mass distribution with an almost constant surface density out to a truncation radius of 139 pc. These properties do not resemble any known astronomical object. However, if the object is dark matter dominated, its structure is incompatible with cold dark matter models but may be compatible with a self-interacting dark-matter halo where the central region has collapsed to form a black hole. This detection could thus carry substantial implications for our current understanding of dark matter.

Seed of supermassive black hole

- little red dots ($z = 4$-11 ; $M_{\rm BH} = 10^{6\text{-}8}\,M_\odot$; $M_{\rm BH}/M_* = 10^{-3}$-10^{-1}) by JWST

- gravothermal collapse + Bondi accretion

- dissipation process would make Bondi accretion Eddington-limited

Feng, Yu and Zhong, arXiv:2506.17641

Contents

Self-interacting dark matter

- core formation in halos

How to find SIDM cross section

- beyond-Born approximation (perturbation)

Dissipative SIDM

- gravothermal collapse

How to find bremsstrahlung cross section

- distorted-wave Born approximation

Setup

Massive dark photon + darkly charged dark-matter fermion

AK and Kuwahara, in progress

$$H = H_{0A'} + H_{0\chi} + V$$

$$H_{0A'} = \sum_{\lambda} \int \frac{d^3k}{(2\pi)^3} \omega_k a^{\dagger}(\vec{k}, \lambda) a(\vec{k}, \lambda)$$

- 2nd quantized (field expanded with plane waves)

$$H_{0\chi} = \sum_n \frac{\vec{p}_n^{\,2}}{2m_n} + \frac{q_1 q_2 \alpha_\chi}{|\vec{x}_1 - \vec{x}_2|} e^{-m_{A'}|\vec{x}_1 - \vec{x}_2|}$$

- 1st quantized and including potential (distorted wave)

$$V = \sum_n \left(q_n e_\chi \phi(\vec{x}_n, t) - \frac{q_n e_\chi}{2m_n} \left[\vec{A}(\vec{x}_n, t) \cdot \vec{p}_n + \vec{p}_n \cdot \vec{A}(\vec{x}_n, t) \right] + \frac{q_n^2 e_\chi^2}{2m_n} \vec{A}(\vec{x}_n, t) \cdot \vec{A}(\vec{x}_n, t) \right)$$

S and T matrices

Distorted-wave Born approximation

AK and Kuwahara, in progress

$$\mathcal{S}_{\text{brem}} = -(2\pi)^4 i\delta(E - E' - \omega_k)\delta^3(\vec{P} - \vec{P}' - \vec{k}) \sum_n q_n e_\chi \left(e^{0*}(\vec{k}, \lambda) D_n^0 - \vec{e}^*(\vec{k}, \lambda) \cdot \vec{D}_n \right)$$

- dipole approximation good for non-relativistic scattering

$$\vec{P} = \vec{p}_1 + \vec{p}_2$$

$$\vec{p} = \frac{1}{m_2}\vec{p}_2 - \frac{1}{m_1}\vec{p}_1$$

$$E = \frac{1}{2M}\vec{P}^2 + \frac{1}{2\mu}\vec{p}^2$$

$$D_1^0 \simeq i\frac{1}{m_1\omega_k^2}\vec{k} \cdot \vec{W} \qquad D_2^0 \simeq -i\frac{1}{m_2\omega_k^2}\vec{k} \cdot \vec{W}$$

$$\vec{D}_1 \simeq i\frac{1}{m_1\omega_k}\vec{W} \qquad \vec{D}_2 \simeq -i\frac{1}{m_2\omega_k}\vec{W}$$

$\omega_k D_n^0 - \vec{k} \cdot \vec{D}_n = 0$ - current conservation

$$\vec{W} = \langle \vec{p}' | \vec{\nabla} V(r) | \vec{p} \rangle = \int d^3r \psi^*_{\text{out},\vec{p}'}(\vec{r}) \left[\vec{\nabla} V(r) \right] \psi_{\text{in},\vec{p}}(\vec{r})$$

$$\psi_{\text{in},\vec{p}}(\vec{r}) \to e^{i\vec{p}\cdot\vec{r}} + f(\vec{p})\frac{e^{ipr}}{r} \qquad \psi_{\text{out},\vec{p}}(\vec{r}) = \psi^*_{\text{in},-\vec{p}}(\vec{r}) \to e^{i\vec{p}\cdot\vec{r}} + f(-\vec{p})^*\frac{e^{-ipr}}{r}$$

Differential cross section

For same-mass particles

AK and Kuwahara, in progress

$$d\sigma_{\rm brem} = 4\alpha_\chi(q_1 - q_2)^2 \frac{|\vec{p}'|}{|\vec{p}|}\frac{|\vec{k}|}{\omega_k^4}\left(\omega_k^2 - \frac{1}{3}\vec{k}^2\right)(4\pi)W_2 d\omega_k$$

$$(4\pi)^4 W_2 = \int d\Omega_{\hat{p}'}|\vec{W}|^2$$

Undistorted-wave Born approximation

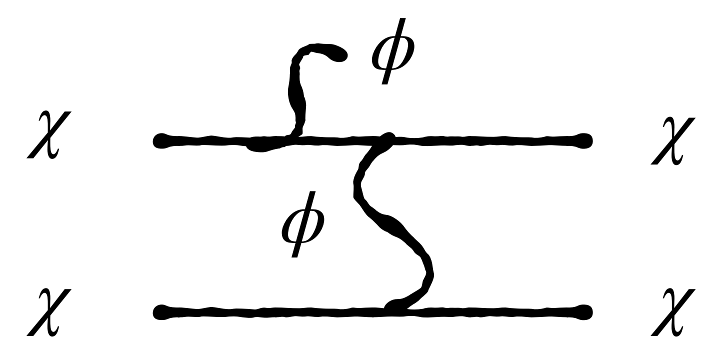

$$\vec{W} \simeq \int d^3r e^{i\vec{q}\cdot\vec{r}}\,\vec{\nabla}V(r) = -i\vec{q}\int d^3r e^{i\vec{q}\cdot\vec{r}}V$$

- Fourier transformation

$$(4\pi)W_2 \simeq \frac{(q_1 q_2 \alpha_\chi)^2}{2}\left[-\frac{2m_{A'}^2}{[(|\vec{p}|+|\vec{p}'|)^2+m_{A'}^2][(|\vec{p}|-|\vec{p}'|)^2+m_{A'}^2]} - \frac{1}{2|\vec{p}||\vec{p}'|}\ln\frac{(|\vec{p}|-|\vec{p}'|)^2+m_{A'}^2}{(|\vec{p}|+|\vec{p}'|)^2+m_{A'}^2}\right]$$

Differential cross section

AK and Kuwahara, in progress

Distorted-wave Born approximation

$$(4\pi)W_2 = \sum_{\ell} \left[(\ell+1) I_{\ell,+}^2 + \ell I_{\ell,-}^2 \right]$$

$$I_{\ell,+} = \int dr r^2 R_{p',\ell+1}(r) V'(r) R_{p,\ell}(r)$$

$$I_{\ell,-} = \int dr r^2 R_{p',\ell-1}(r) V'(r) R_{p,\ell}(r)$$

Undistorted vs distorted

- three regimes again

Tulin, Yu and Zurek, PRD, 2013

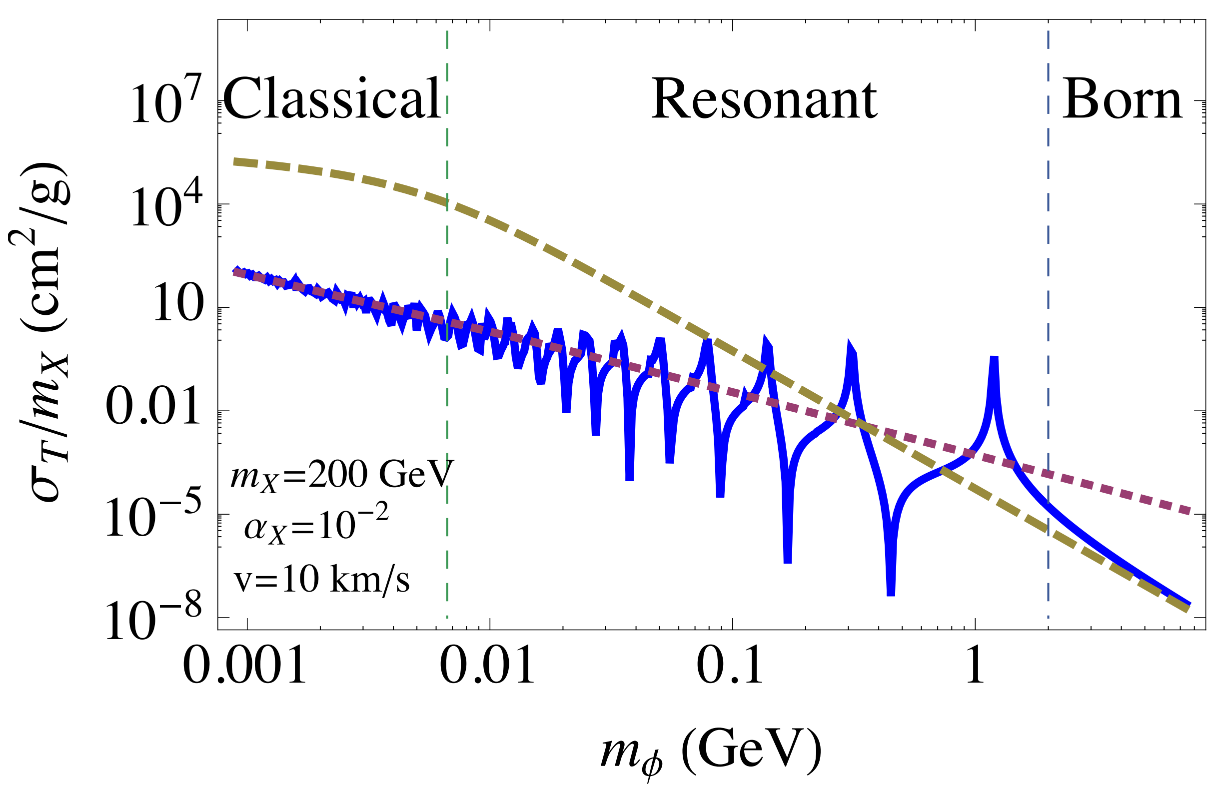

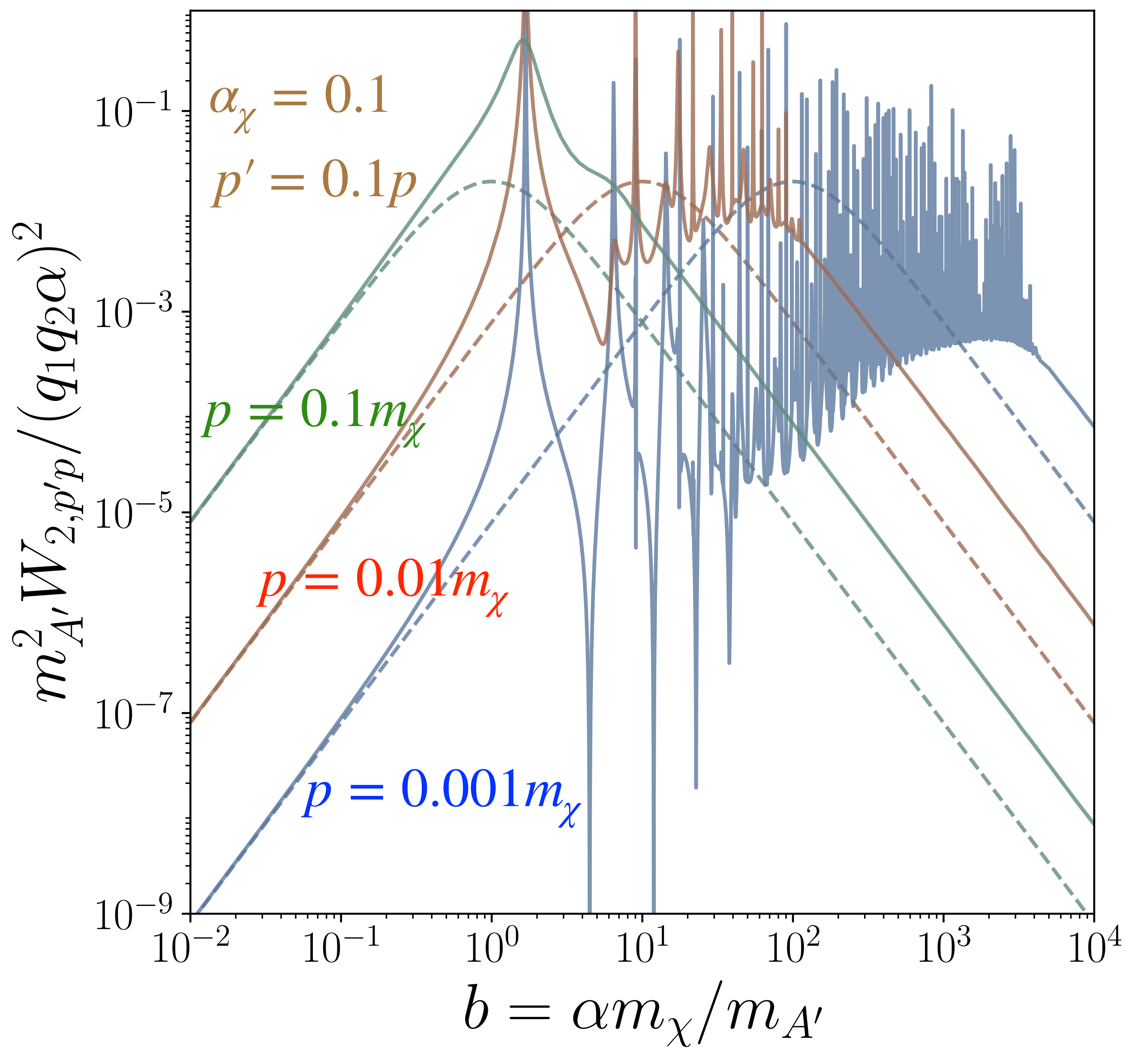

Summary

(Dissipative) self-interacting dark matter

- not only core formation but also gravothermal collapse
- collapsed objects (black hole) are detectable

Cross-section computation

- even a perturbative relativistic theory leads to non-perturbative non-relativistic phenomenology
- distorted-wave Born approximation is required
- any way to simplify computation?

Thank you

Underlying physics of SIDM

How a core forms

- heat transfer inside a halo

- iso-thermal (equal temperature) region forms

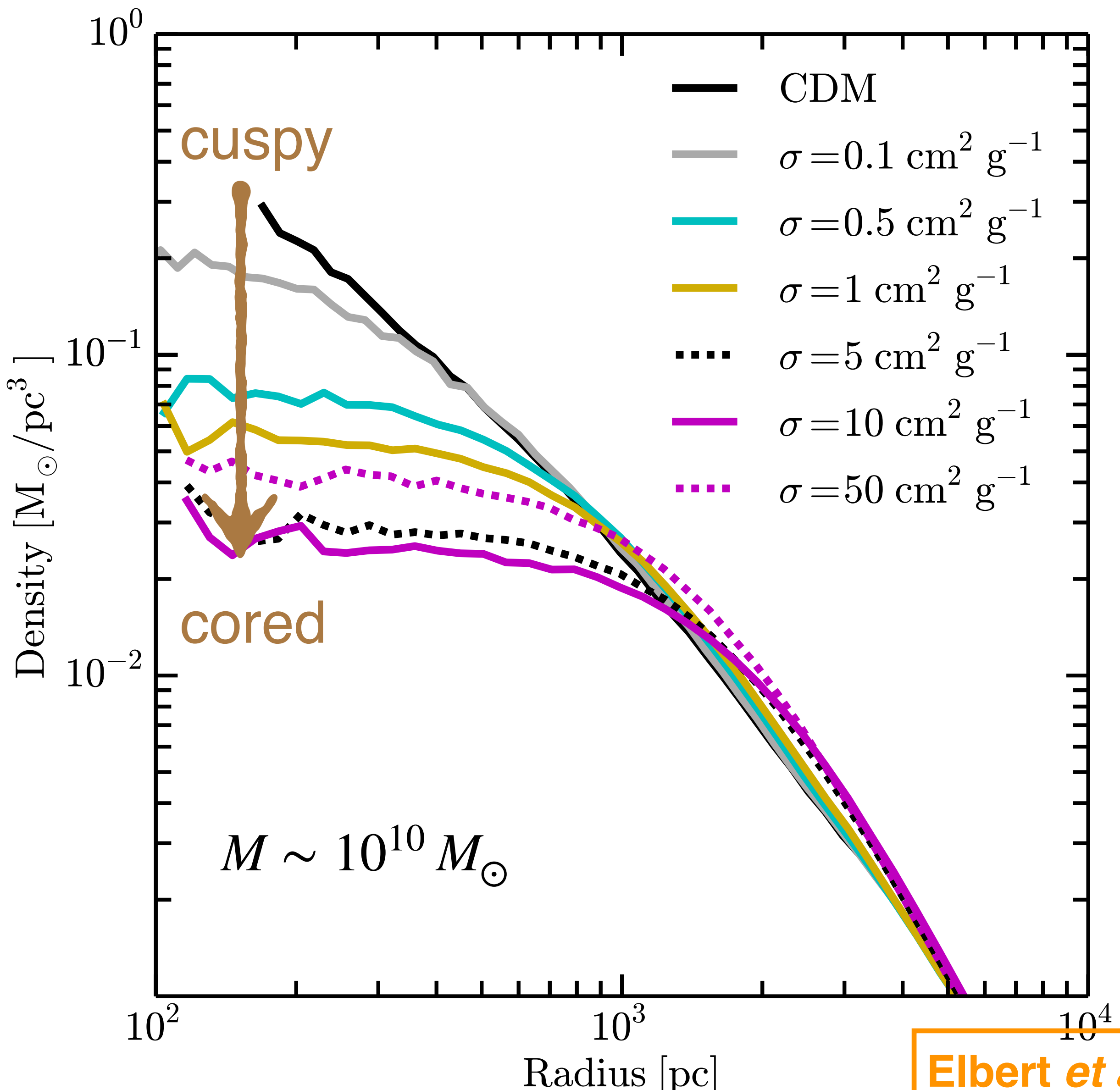

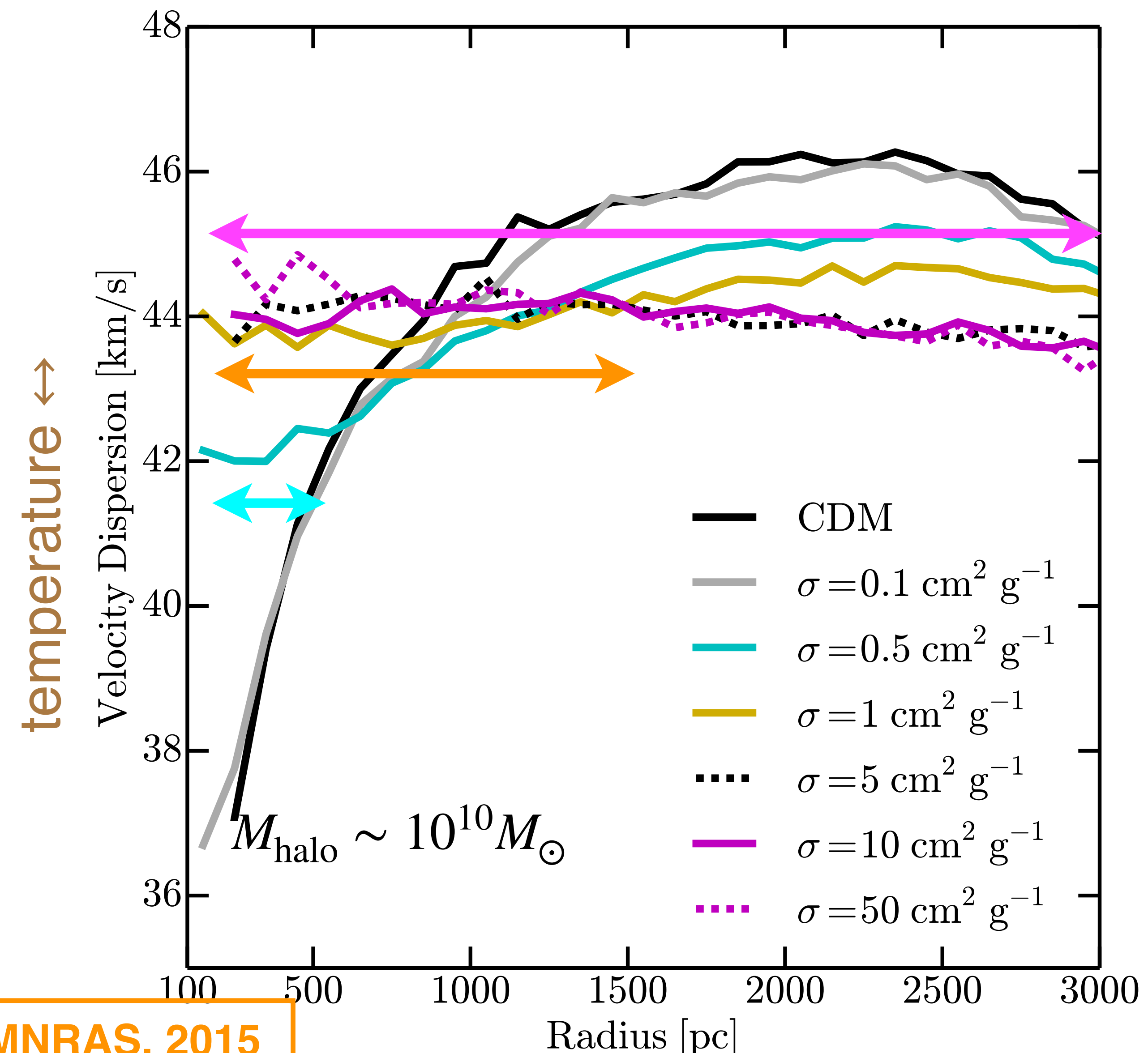

Elbert *et al.*, MNRAS, 2015

Sommerfeld enhancement

Distortion of wave function

- multiple exchanges of a mediator

- non-perturbative but described by the Schrödinger equation (later)

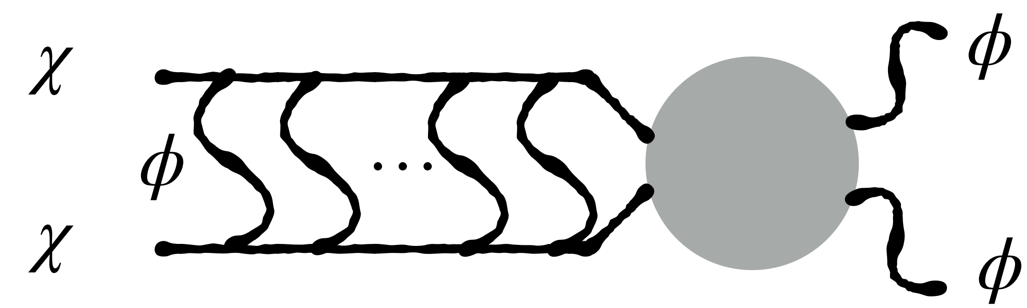

Enhanced annihilation

- annihilation cross section is enhanced at low velocity

$$(\sigma_{\mathrm{ann}} v_{\mathrm{rel}}) = \mathrm{S}(\sigma_{\mathrm{ann}}^{(0)} v_{\mathrm{rel}})$$

- without potential

- Sommerfeld enhancement factor

- larger cross section in the late Universe than the thermal one

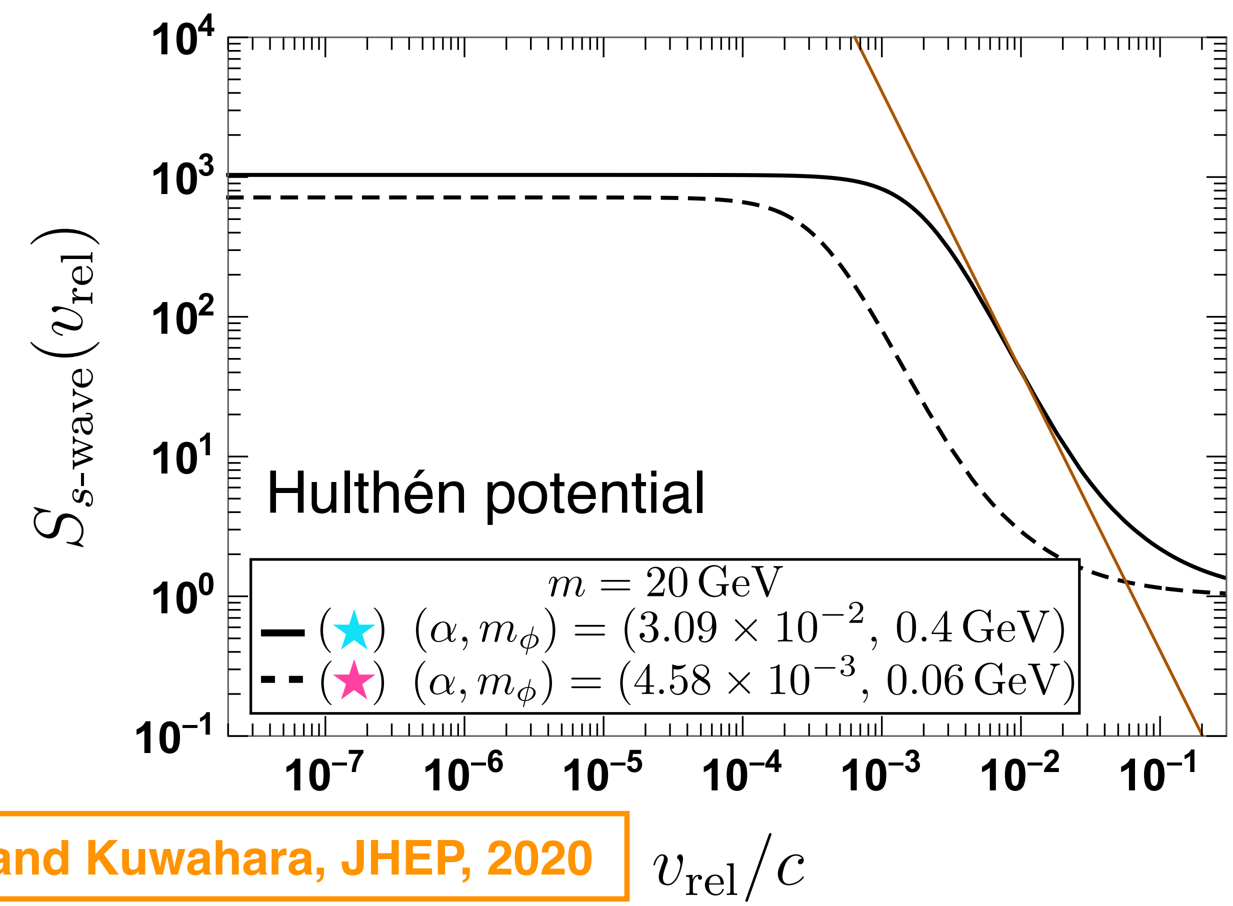

AK, Kim and Kuwahara, JHEP, 2020

Indirect detection

Canonical cross section

- thermal freeze-out (annihilation in the early Universe) $v_{\rm rel} \simeq 1/2$

$$\Omega h^2 = 0.1 \times \frac{3\times10^{-26}\,{\rm cm^3/s}}{\langle\sigma_{\rm ann} v\rangle}$$

- requires a weak-scale annihilation cross section

$$\langle\sigma_{\rm ann} v\rangle \simeq 1\,{\rm pb}\times c$$

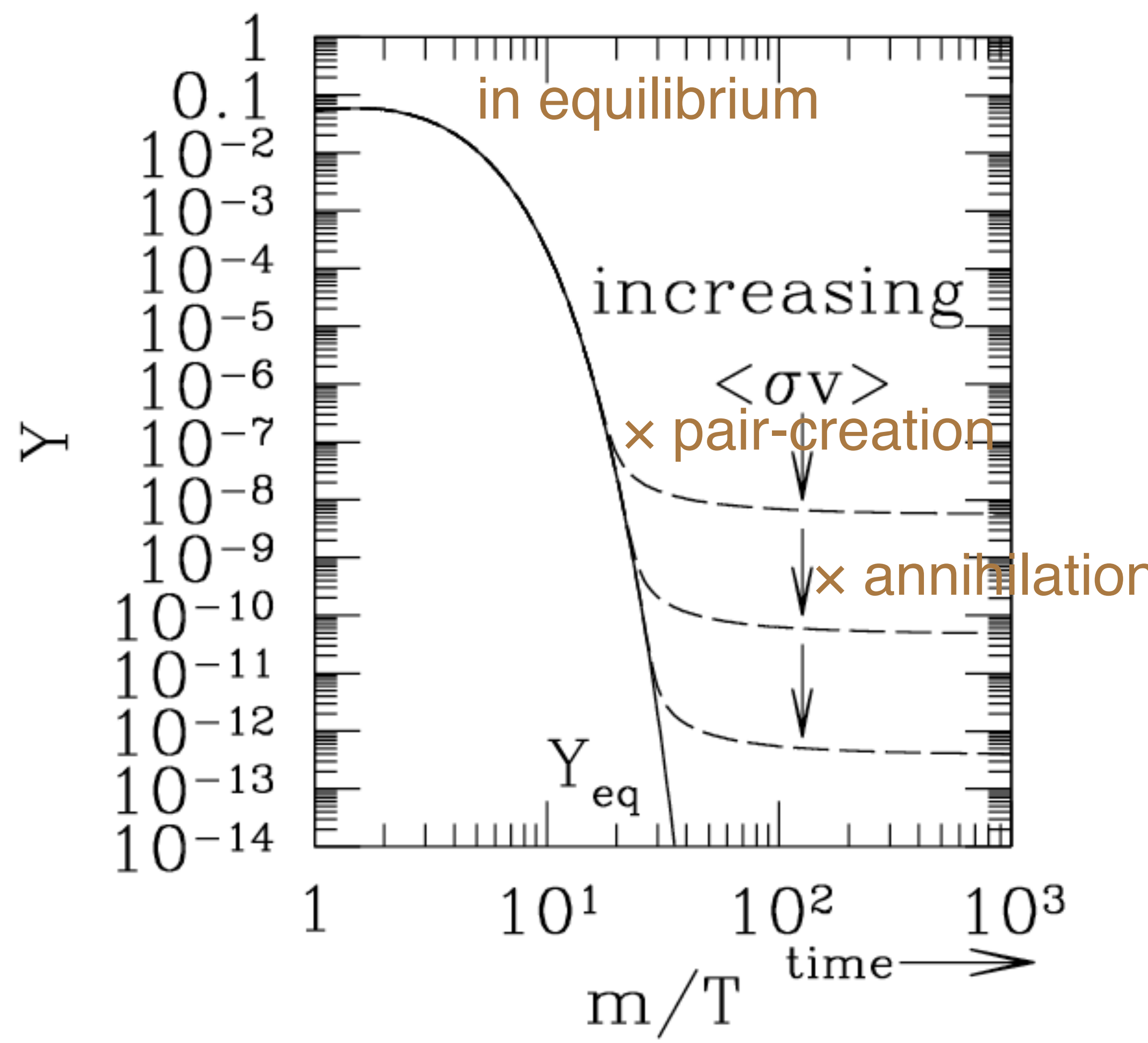

CMB constraints

- energy deposit around the last scattering

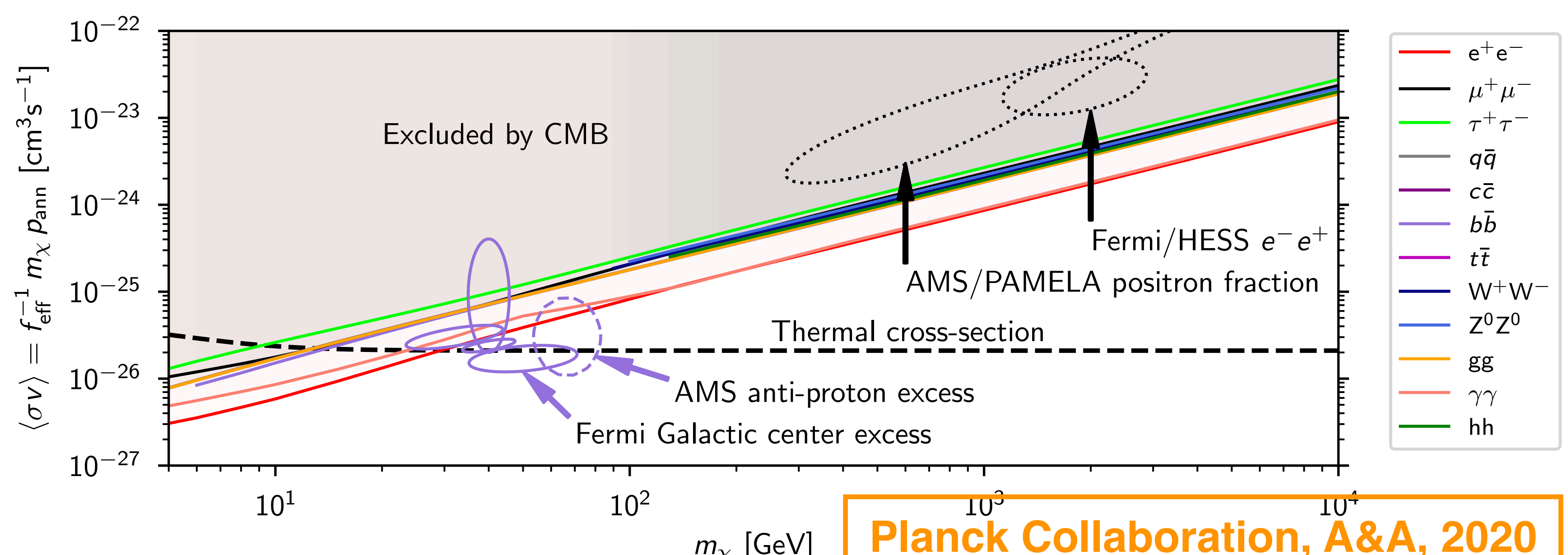

Planck Collaboration, A&A, 2020

Correlation

Bringmann, Kahlhoefer, Schmidt-Hoberg and Walia, JHEP, 2020

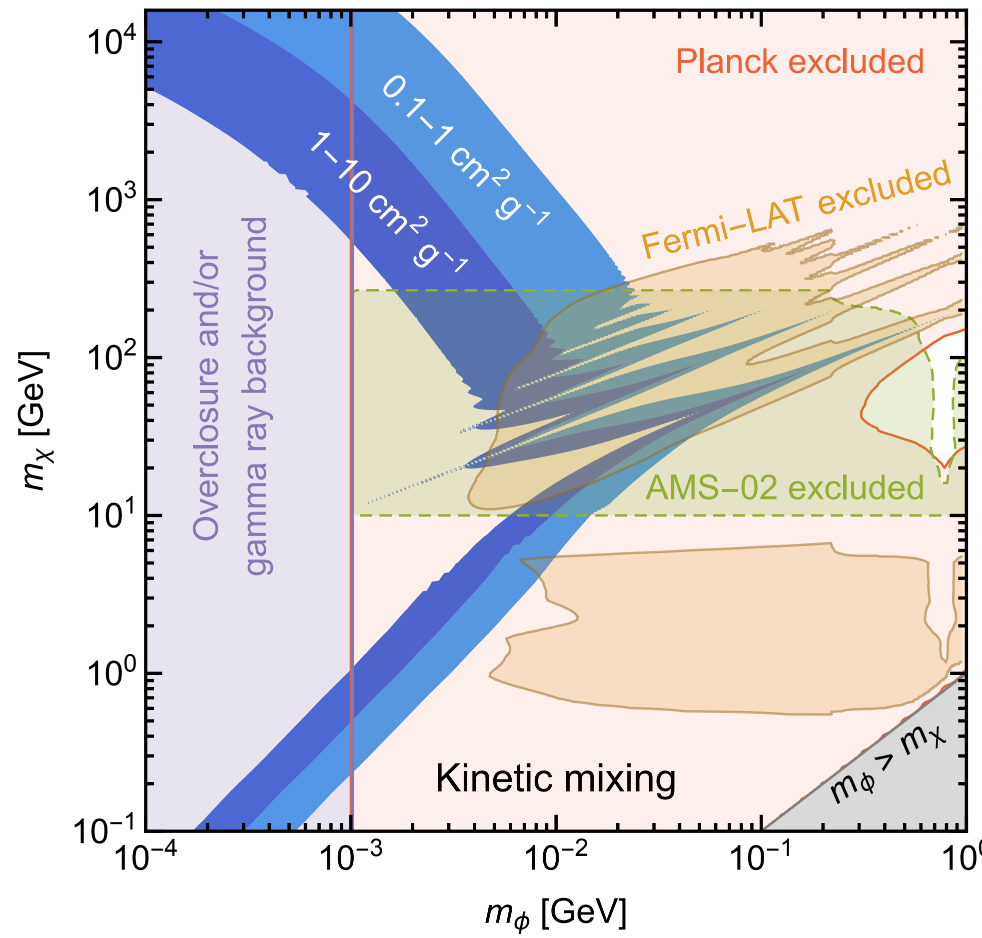

Sommerfeld enhancement and self-scattering

- correlated
  - resonant enhancement occurs at the same parameter point
    - zero-energy resonances (later)
- main obstacle in SIDM model building

- dark photon

$$a = \frac{v_{\rm rel}}{2\alpha_\chi}$$

$$b = \frac{\alpha_\chi m_\chi}{m_\phi}$$

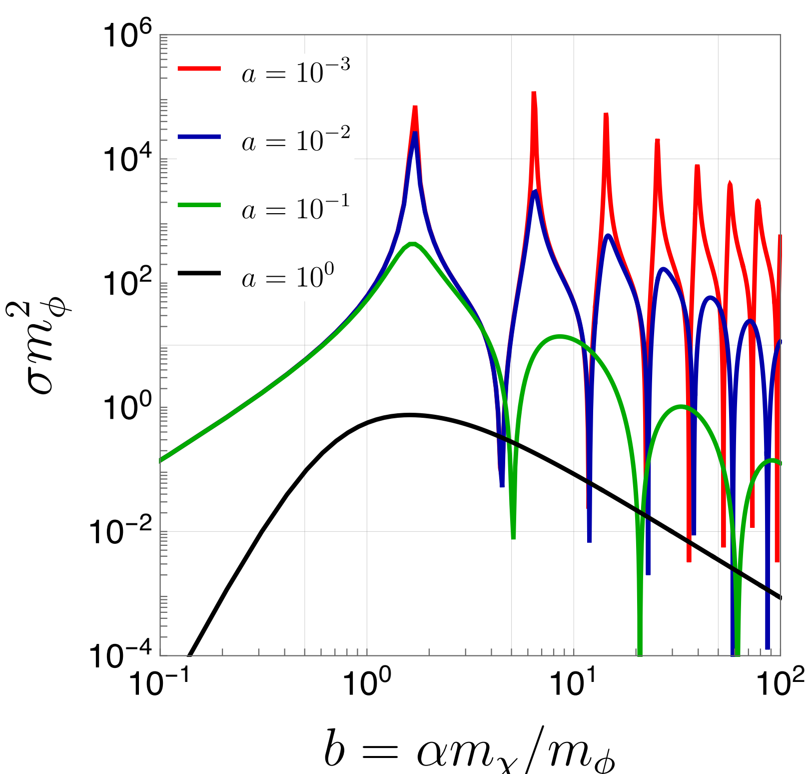

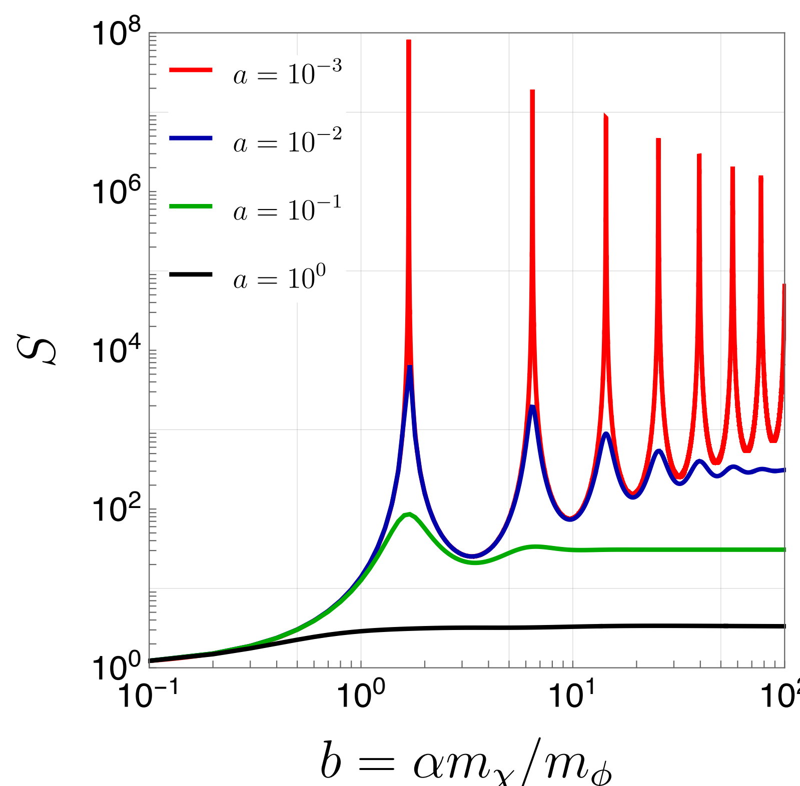

AK, Kuwahara and Patel, JHEP, 2023

Correlation

Zero-energy resonances

- resonant enhancement occur

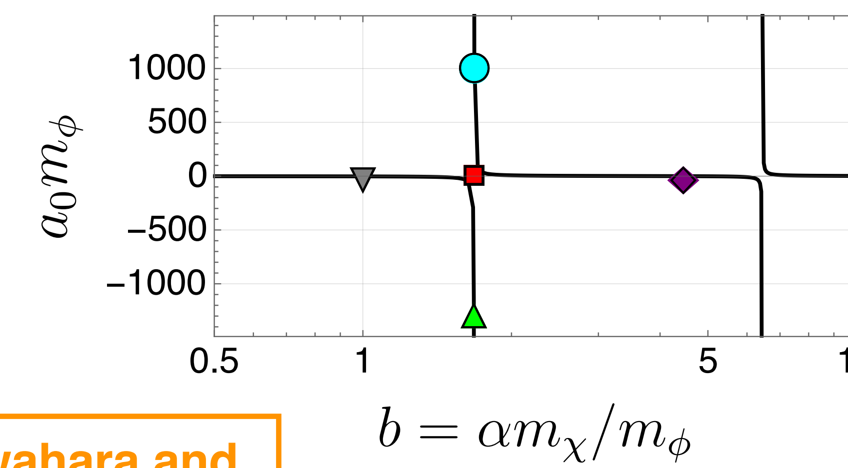

AK, Kuwahara and Patel, JHEP, 2023

Effective range theory

$$k^{2\ell+1}\cot\delta_\ell \to -\frac{1}{a_\ell^{2\ell+1}} + \frac{1}{2r_{e,\ell}^{2\ell-1}}k^2$$

- scattering length
- effective range

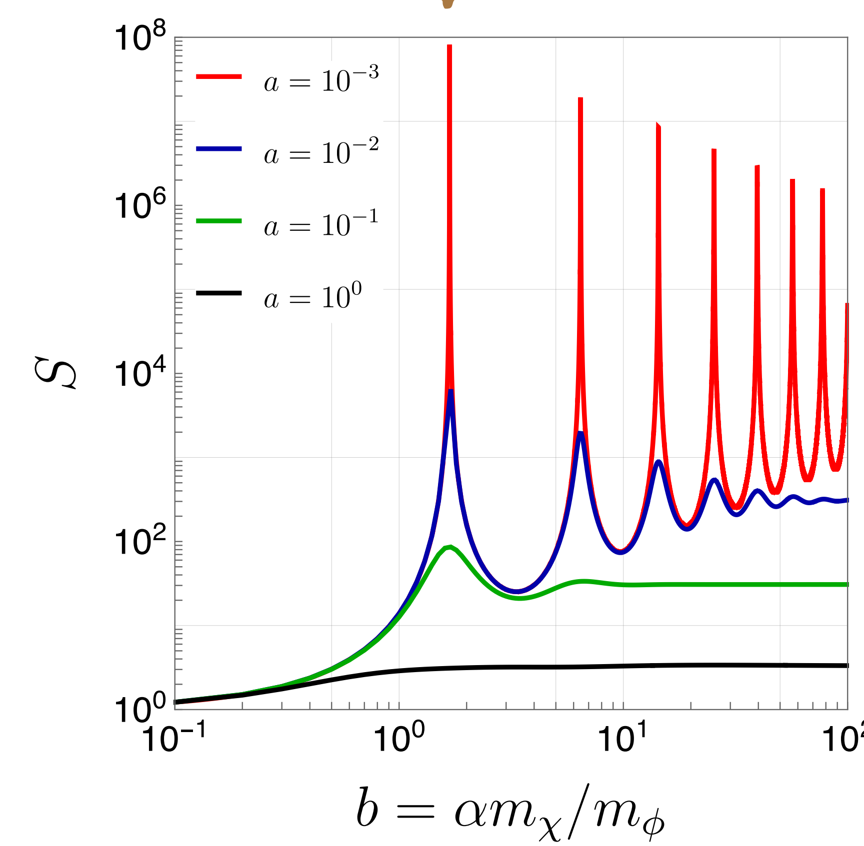

- on resonance $a_0 \to \infty$
- shallow virtual level
  - non-normalizable
- shallow bound state
  - pole of scattering amplitude

Jost function

How to find $R_{k,\ell}(r)$ in practice?

AK, Kuwahara and Patel, JHEP, 2023

AK, Matsumoto and Patel and Watanabe, in progress

- "initial" condition given at the origin (regularity)

$$\mathscr{R}_{p,\ell}(r) \to p j_\ell(pr) \approx p \frac{(pr)^\ell}{(2\ell+1)!!} \quad r \to 0$$

- radial Schrödinger equation

$$\left[\frac{1}{r^2}\frac{d}{dr}r^2\frac{d}{dr} + p^2 - \frac{\ell(\ell+1)}{r^2} - 2\mu V(r)\right]\mathscr{R}_{p,\ell}(r) = 0$$

- asymptotic behavior of solution

$$\mathscr{R}_{p,\ell}(r) \to \frac{i}{2r}\left[\mathscr{J}_\ell(p)e^{-i\left(pr - \frac{1}{2}\ell\pi\right)} - \mathscr{J}_\ell(-p)e^{i\left(pr - \frac{1}{2}\ell\pi\right)}\right] \quad r \to \infty$$

- Jost function

- by comparing asymptotic behavior

$$R_{p,\ell}(r) = \frac{1}{|\mathscr{J}_\ell(p)|}\mathscr{R}_{p,\ell}(r) \qquad S_\ell(p) = e^{2i\delta_\ell(p)} = \frac{\mathscr{J}_\ell(-p)}{\mathscr{J}_\ell(p)}$$

Analytic property

Complex momentum squared

$$\Gamma_\ell(k^2) = \frac{1}{\mathcal{J}_\ell(k^2)}$$

- “real” complex function

$$\Gamma^*_\ell(k^2) = \Gamma_\ell(k^{2*})$$

- brach cut along real (physical) axis

$$\Gamma_\ell(k^2 + i\epsilon) = e^{2i\delta_\ell(k)}\Gamma_\ell(k^2 - i\epsilon)$$

- real k^2

- known as Watson theorem (kind of optical theorem)

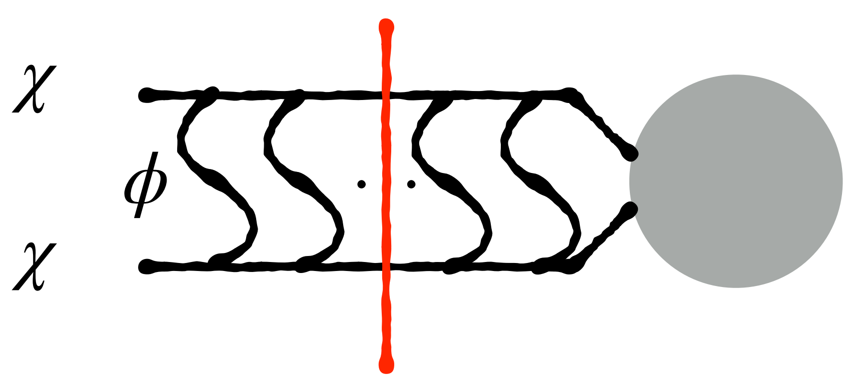

- bound states

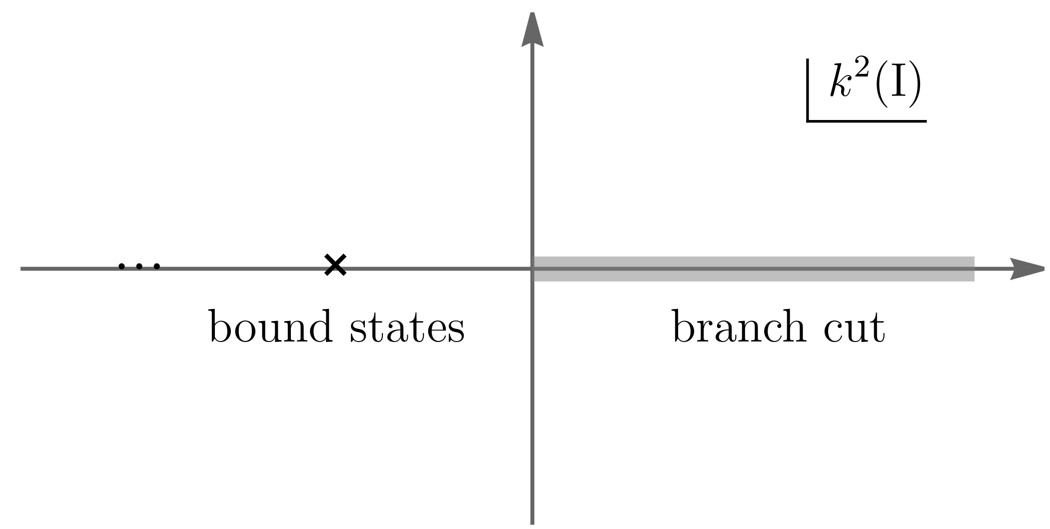

- 1st Riemann sheet $\mathrm{Im}(k) > 0$

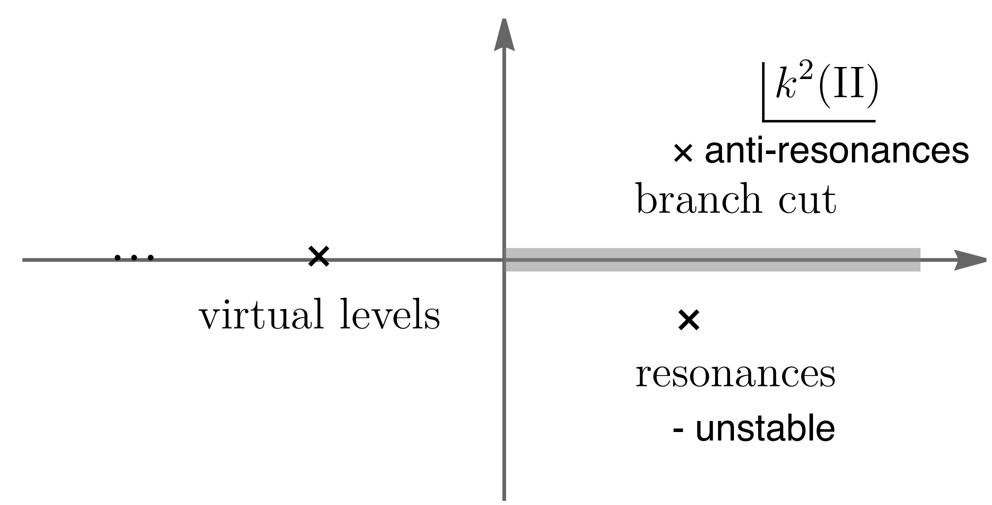

- 2nd Riemann sheet $\mathrm{Im}(k) < 0$

Omnès solution

AK, Kuwahara and Patel, JHEP, 2023

Annihilation matrix element

- analytic continuation to complex momentum

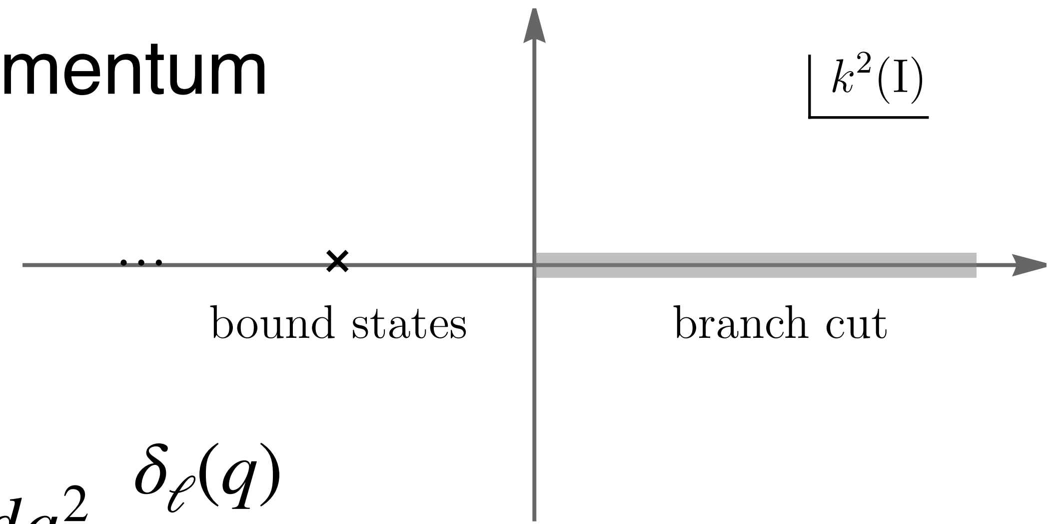

$$\Gamma_\ell(k^2) = \frac{1}{\mathcal{J}_\ell(k^2)} = \Omega_\ell(k^2) F_\ell(k^2)$$

$$\Omega_\ell(k^2) = \exp[\omega_\ell(k^2)] \qquad \omega_\ell(k^2) = \frac{1}{\pi}\int_0^\infty dq^2 \frac{\delta_\ell(q)}{q^2 - k^2}$$

- reproducing the brunch cut

$$F_\ell(k^2) = \prod_{b_\ell} \frac{k^2}{k^2 + \kappa_{b,\ell}^2}$$

- rational function reproducing bound-state poles
- numerator is chosen so that no singularity at $k \to 0$
  - discussed next

Omnès solution

Levinson theorem

Weinberg, "Lectures on Quantum Mechanics"

- # of bound states is given by phase shift

$$\delta_\ell(k \to 0) - \delta_\ell(k \to \infty) = \left[\#b_\ell \left(+\frac{1}{2} \right) \right] \pi$$

- excluding virtual levels

- zero in our normalization

- only for s-wave zero-energy resonances

- underlying idea
  - consider the system confined in a large sphere

$$R_{k\ell}(r) \to \frac{\sin(kr - \frac{1}{2}\ell\pi + \delta_\ell)}{r}$$

$$r \to \infty$$

$$k > 0$$

$$kR - \frac{1}{2}\ell\pi + \delta_\ell = n\pi$$

$$n = 0, \pm 1, \pm 2 \ldots$$

- scattering states are discretized (countable infinity)

- decrease in # of scattering states = # of bound states
  - total number does not change

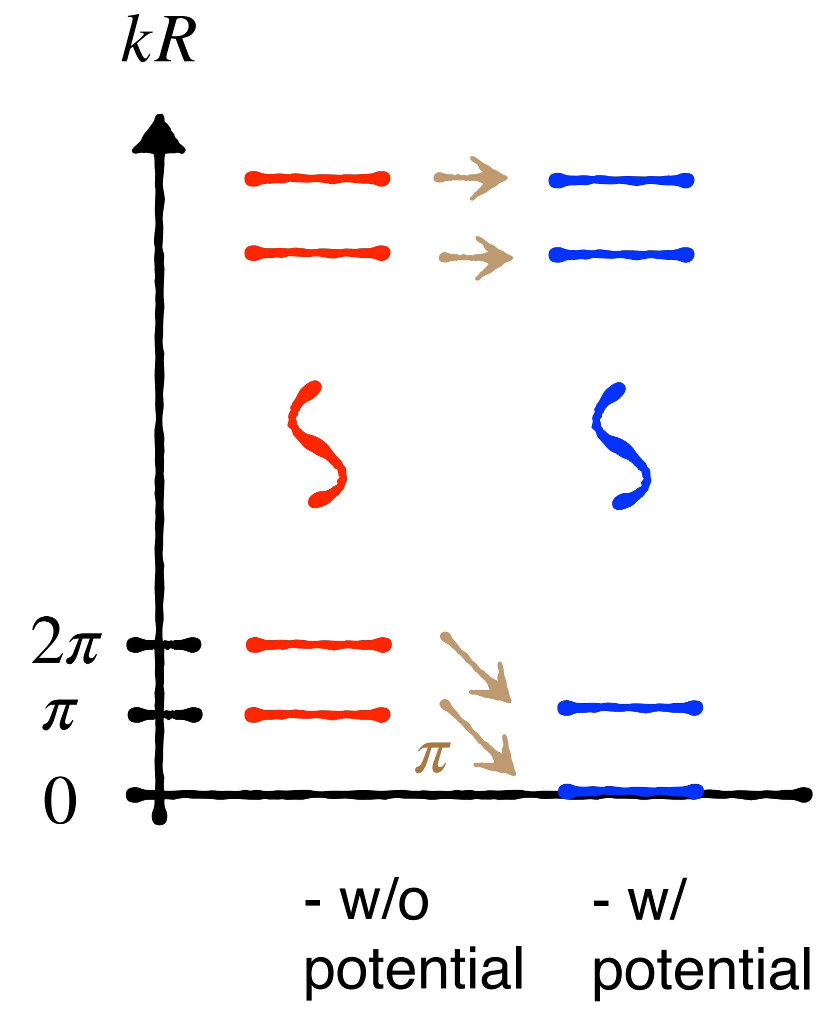

Omnès solution

Levinson theorem

Weinberg, "Lectures on Quantum Mechanics"

- # of bound states is given by phase shift

$$\delta_\ell(k \to 0) - \delta_\ell(k \to \infty) = \left[\#b_\ell \left(+\frac{1}{2}\right)\right] \pi$$

- excluding virtual levels

- zero in our normalization

- only for s-wave zero-energy resonances

$k \to 0$ behavior

- Omnès function is singular with the power of # of bound states

$$\mathrm{Re}[\omega_\ell(k^2 + i\epsilon)] = \frac{1}{\pi} ⨍_0^\infty dq^2 \frac{\delta_\ell(q)}{q^2 - k^2} \quad \to -\left[\#b_\ell \left(+\frac{1}{2}\right)\right] \ln(k^2/\Lambda^2) \quad k \to 0$$

$$\Gamma_\ell(k^2 + i\epsilon) = \exp[\omega_\ell(k^2 + i\epsilon)] F_\ell(k^2) \quad \propto \frac{F_\ell(k^2)}{k^{2\#b_\ell(+1)}} \quad k \to 0$$

$$F_\ell(k^2) = \prod_{b_\ell} \frac{k^2}{k^2 + \kappa_{b,\ell}^2} \propto k^{2\#b_\ell} \quad k \to 0$$

Omnès solution

Yukawa potential

AK, Kuwahara and Patel, JHEP, 2023

- s-wave

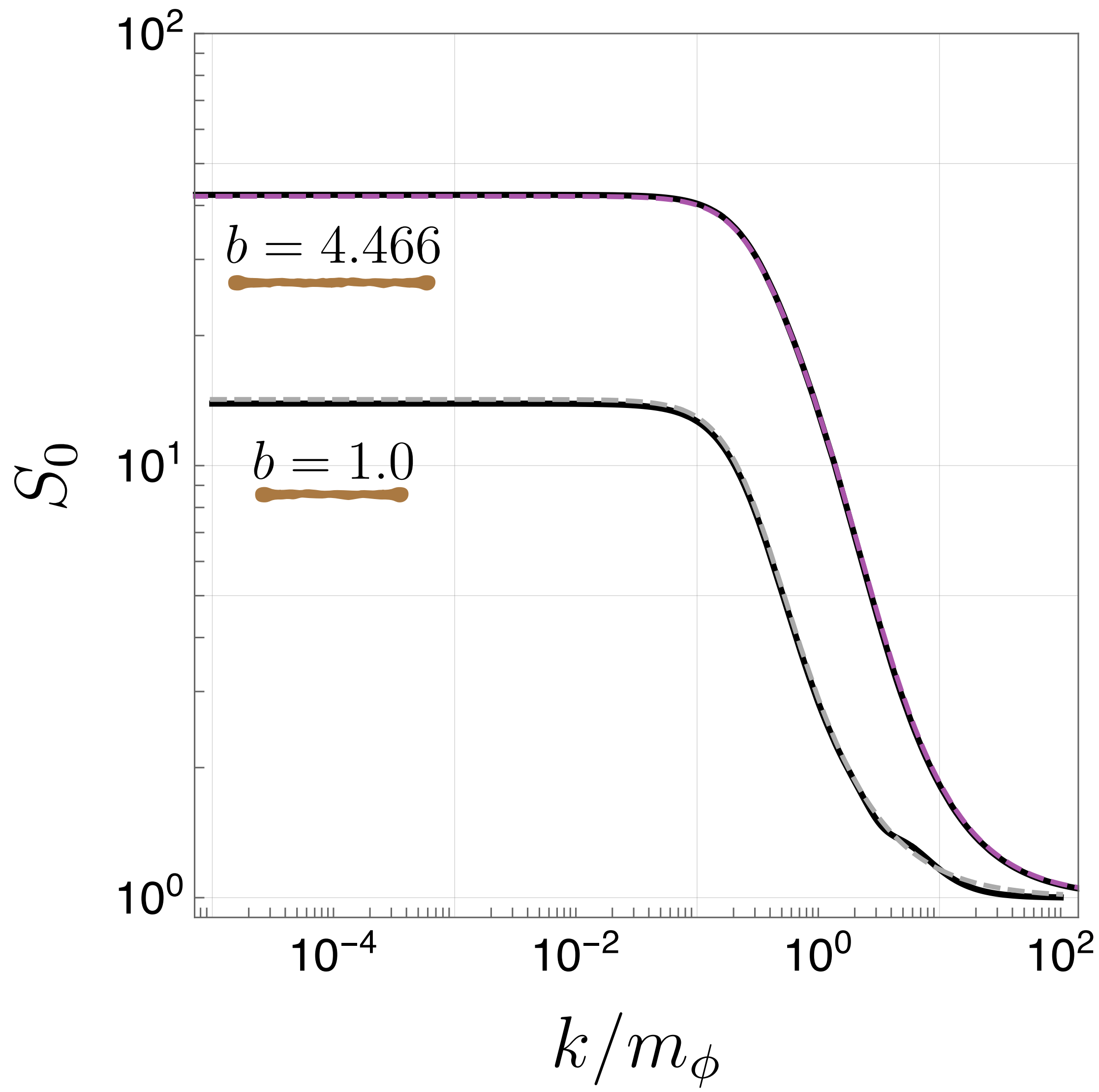

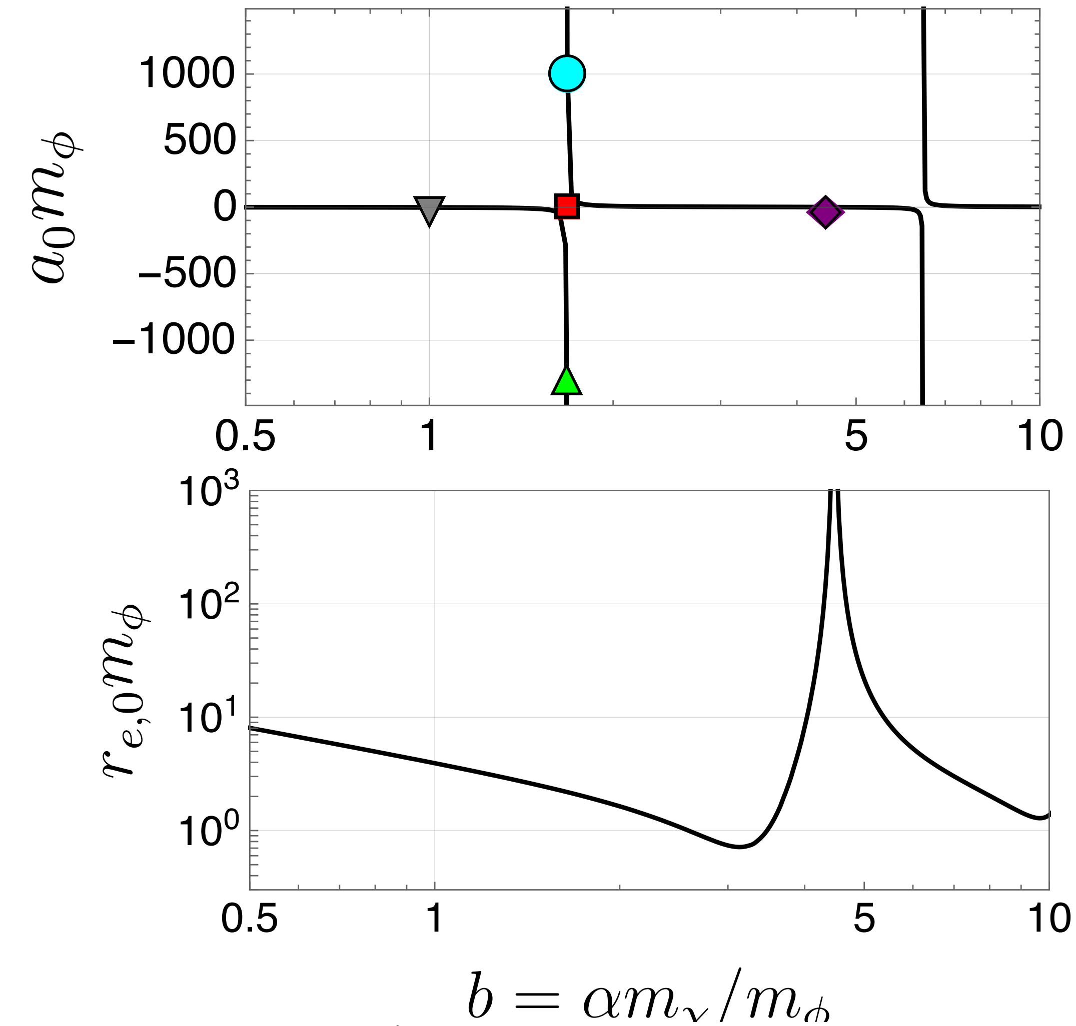

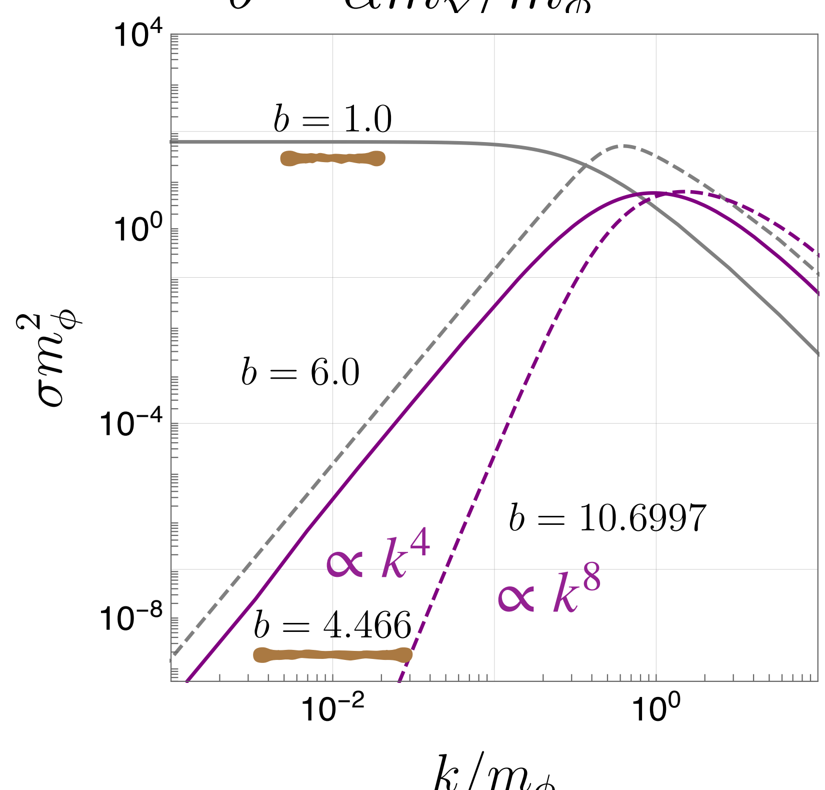

- Omnès solution agrees with direct computation from scattering state

    - with proper $F_0(k^2)$

Around zero-energy resonances

AK, Kuwahara and Patel, JHEP, 2023

S-wave

$$\delta_0(k \to 0) = \left[\#b_0\left(+\frac{1}{2}\right)\right]\pi$$

- on 1st resonance $\#b_0 = 0$

$$k \to 0 \quad \mathrm{Re}[\omega_0(k^2 + i\epsilon)] \to -\frac{1}{2}\ln(r_{e,0}^2 k^2)$$

- only zero energy "virtual" level $F_0(k^2) = 1$

$$k \to 0 \quad \Gamma_0(k^2) = \exp[\omega_0(k^2)]F_0(k^2) \propto \frac{1}{k}$$

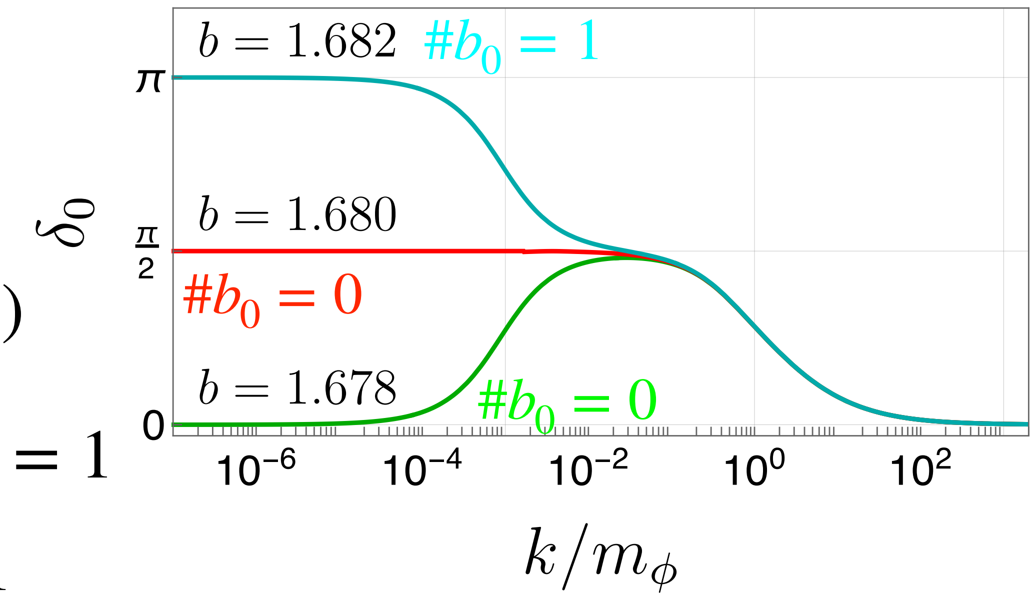

- slightly below the 1st resonance $\#b_0 = 0$
  - no bound state $F_0(k^2) = 1$

- slightly above the 1st resonance $\#b_0 = 1$

$$k \to 0 \quad \mathrm{Re}[\omega_0(k^2 + i\epsilon)] \to -\ln(r_{e,0}^2 k^2)$$

- single bound state $F_0(k^2) = \dfrac{k^2}{k^2 + \kappa_{b,0}^2}$

$$k \to 0 \quad \Gamma_0(k^2) \propto \frac{1}{k^2 + \kappa_{b,0}^2}$$

- saturates at low k

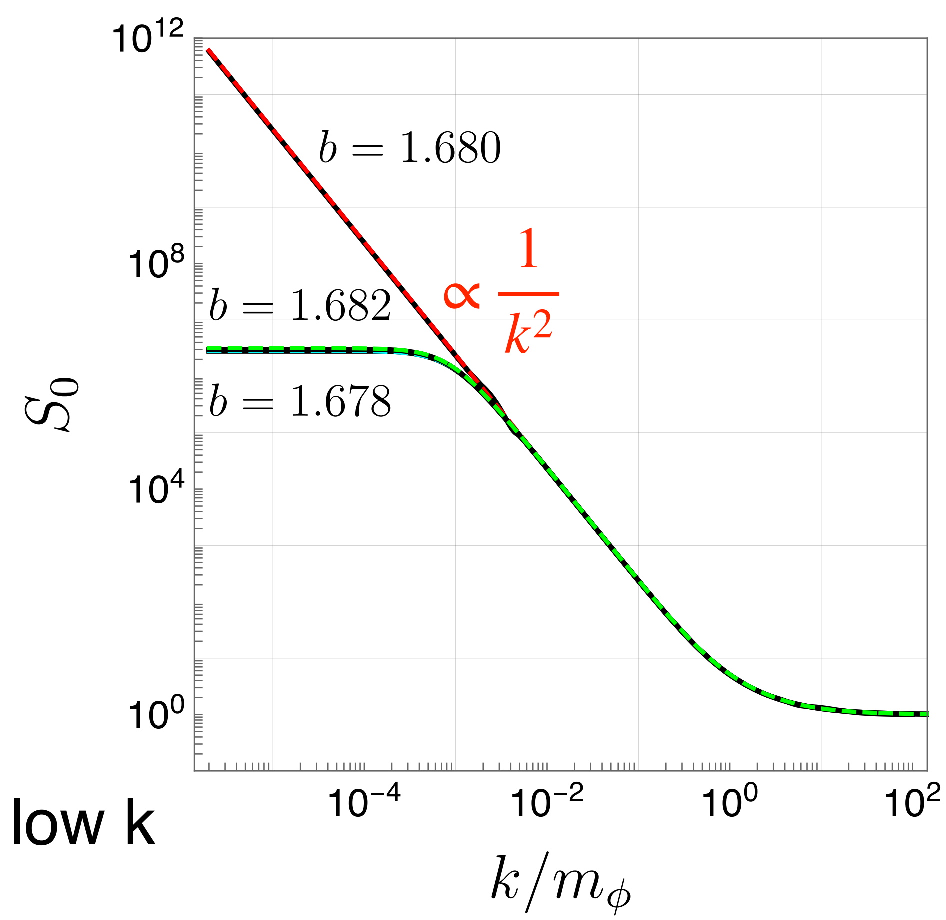

Omnès solution

Yukawa potential

AK, Kuwahara and Patel, JHEP, 2023

- p-wave

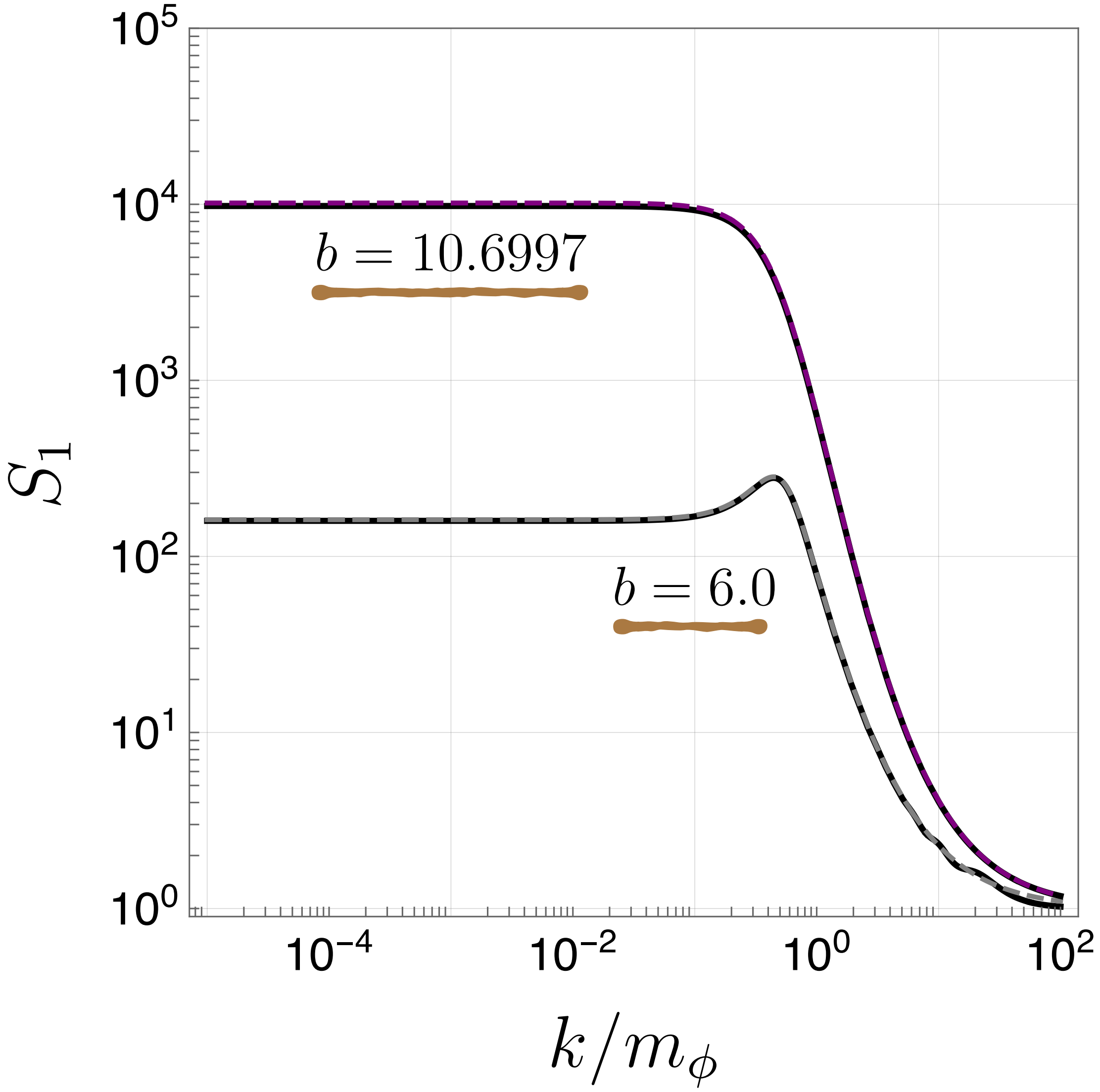

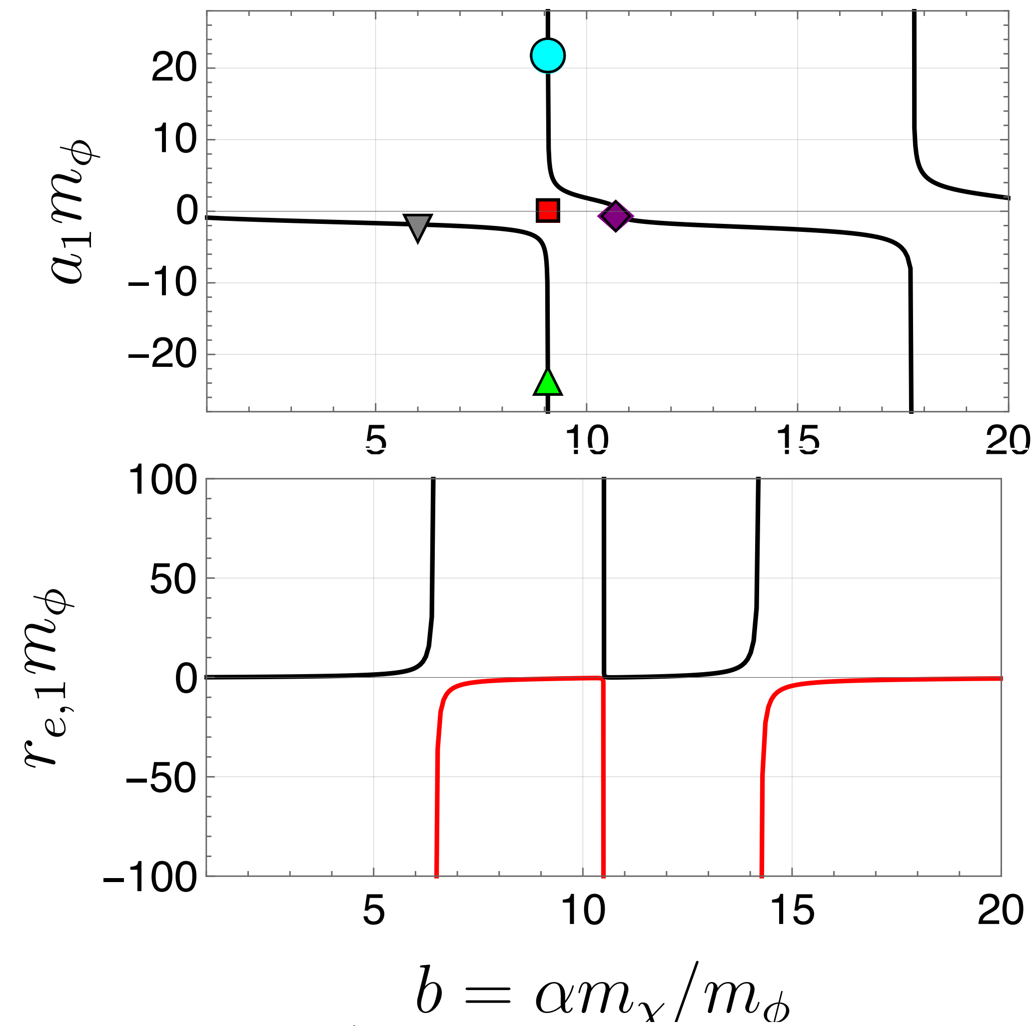

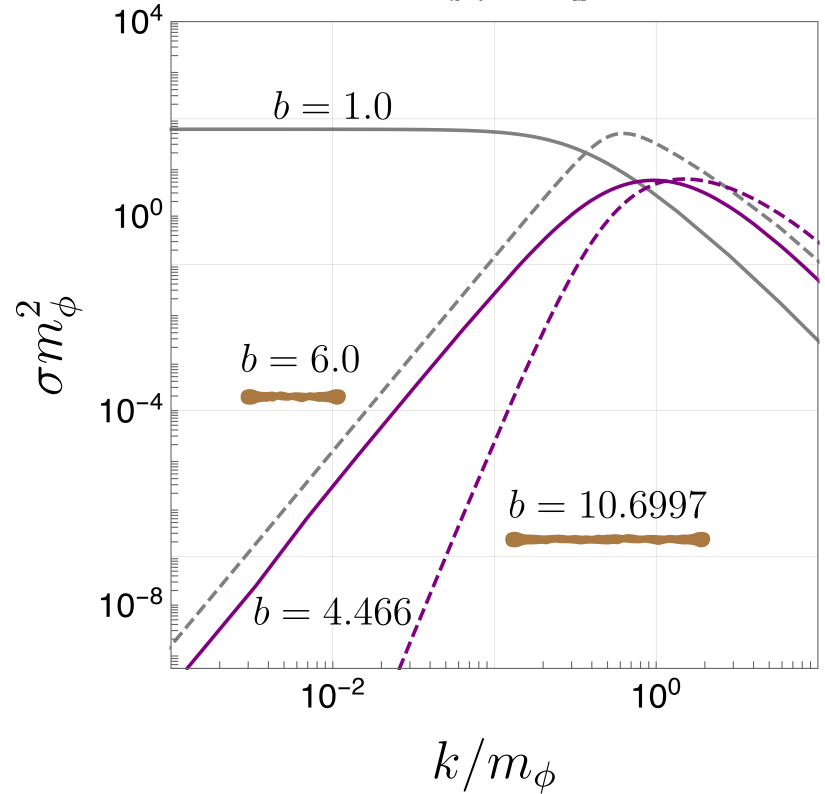

Zero-energy resonances

No cancellation

AK, Kuwahara and Patel, JHEP, 2023

- s-wave 1st resonance $\#b_0 = 0$

$$k \to 0 \quad \mathrm{Re}[\omega_0(k^2 + i\epsilon)] \to -\frac{1}{2}\ln(r_{e,0}^2 k^2)$$

- only zero energy "virtual" level $F_0(k^2) = 1$

$$k \to 0 \quad \Gamma_0(k^2) = \exp[\omega_0(k^2)]F_0(k^2) \propto \frac{1}{k}$$

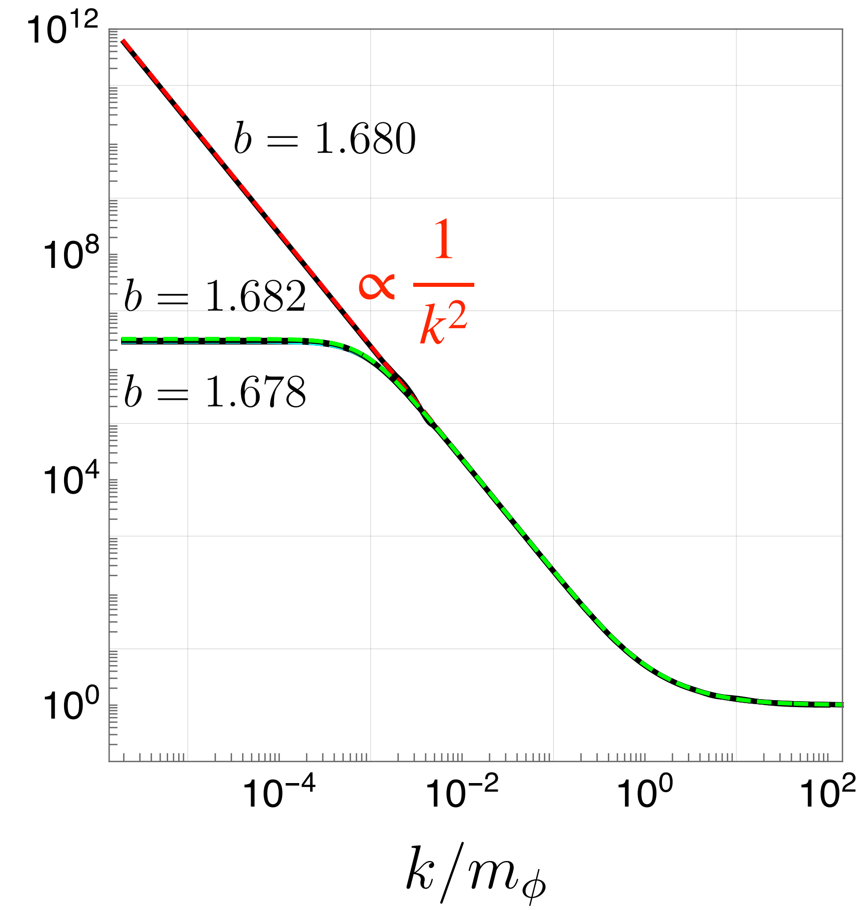

- p-wave 1st resonance $\#b_1 = 1$

$$k \to 0 \quad \mathrm{Re}[\omega_1(k^2)] \to -\ln(r_{e,1}^2 k^2)$$

- zero energy bound state $F_1(k^2) = \frac{k^2}{k^2} = 1$

$$k \to 0 \quad \Gamma_1(k^2) = \exp[\omega_1(k^2)]F_1(k^2) \propto \frac{1}{k^2}$$

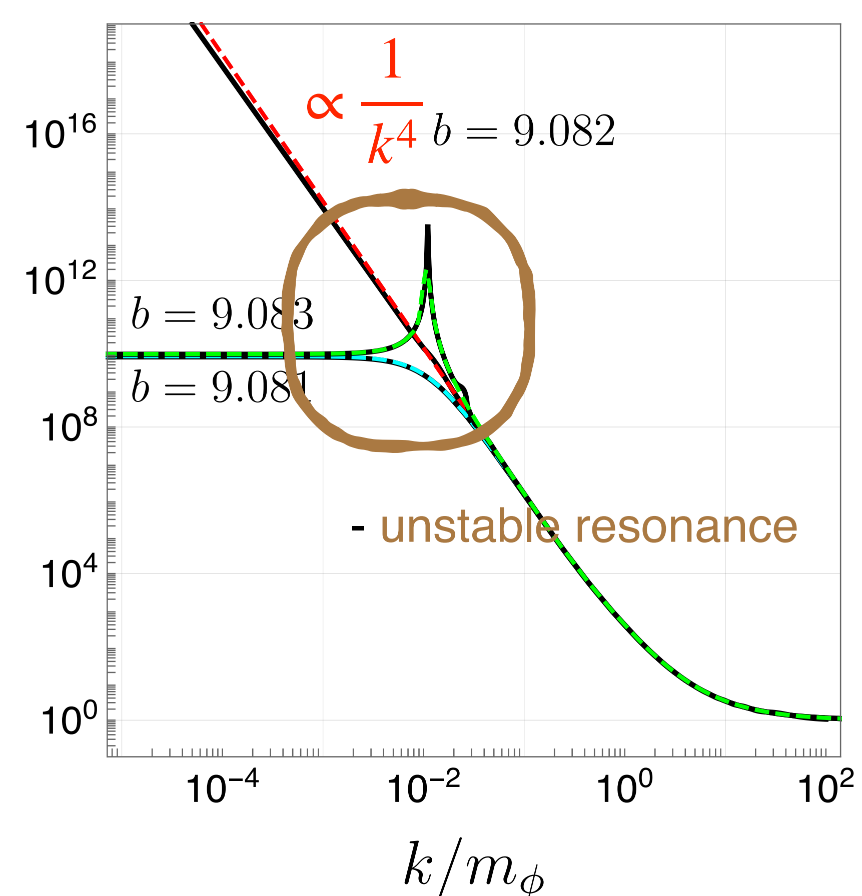

Zero-energy resonances

Unitarity violation

- on s- and p-waves zero-energy resonances, partial-wave Unitarity is violated at low velocity

$$(\sigma_{\ell,\mathrm{ann}} v_{\mathrm{rel}}) = \mathrm{S}_\ell (\sigma^{(0)}_{\ell,\mathrm{ann}} v_{\mathrm{rel}}) \qquad (\sigma^{(0)}_{\ell,\mathrm{ann}} v_{\mathrm{rel}}) \propto k^{2\ell} \qquad (\sigma^{\mathrm{Uni}}_{\ell,\mathrm{ann}} v_{\mathrm{rel}}) = \frac{\pi}{\mu k}$$

$$\mathrm{S}_0(k^2) \propto \frac{1}{k^2} \qquad \mathrm{S}_{\ell \geq 1}(k^2) \propto \frac{1}{k^4}$$

- because we ignored a contact interaction including annihilation when solving the Schrödinger equation $V \supset u\delta^3(\vec{x})$

Self-consistent solution

Blum, Sato and Slatyer, JHEP, 2016

Parikh, Sato and Slatyer, arXiv:2410.18168

AK, Matsumoto and Watanabe, in progress

- incorporating contact interaction is not as easy as one expects

- mathematical fact: there is no bounded wave function if a potential is singular than the centrifugal one

Full scattering state

AK, Matsumoto and Watanabe, in progress

Linear combination of regular and singular solutions

$$\tilde{R}_{k,\ell}(r) = \mathscr{A}_\ell(k)\mathscr{R}_{k,\ell}(r) + \mathscr{B}_\ell(k)\mathscr{S}_{k,\ell}(r)$$ - valid except for the origin

- regular solution we discussed before

- singular solution we introduce now

$$\mathscr{S}_{k,\ell}(r) \to k y_\ell(kr) \approx -k\frac{(2\ell-1)!!}{(kr)^{\ell+1}} \qquad r \to 0$$

$$\mathscr{S}_{k,\ell}(r) \to -\frac{1}{2r}\left[\mathscr{K}_\ell(k)e^{-i\left(kr-\frac{1}{2}\ell\pi\right)} + \mathscr{K}_\ell(-k)e^{i\left(kr-\frac{1}{2}\ell\pi\right)}\right] \qquad r \to \infty$$

- one combination of two unknown coefficients is fixed by requirement of in-coming wave

$$\tilde{R}_{k,\ell}(r) \to \frac{i}{2r}\left[e^{-i\left(kr-\frac{1}{2}\ell\pi\right)} - S_\ell(k)e^{i\left(kr-\frac{1}{2}\ell\pi\right)}\right] \qquad r \to \infty$$

$$\mathscr{A}_\ell(k)\mathscr{J}_\ell(k) + i\mathscr{B}_\ell(k)\mathscr{K}_\ell(k) = 1 \qquad S_\ell(k) = \frac{\mathscr{J}_\ell(-k)}{\mathscr{J}_\ell(k)}\left[1 - i\mathscr{B}_\ell(k)\mathscr{K}_\ell(k)\right] - i\mathscr{B}_\ell(k)\mathscr{K}_\ell(-k)$$

Full scattering state

The other combination is fixed by renormalization condition

$$\mathscr{B}_\ell(k) = \frac{k^{2\ell+1}}{p_\ell(k)\mathscr{J}_\ell(k)} \qquad \tilde{R}_{k,\ell}(r) = \mathscr{B}_\ell(k)\left(\left[p_\ell(k) - k^{2\ell+1}\frac{i\mathscr{K}_\ell(k)}{\mathscr{J}_\ell(k)}\right]\frac{\mathscr{R}_{k,\ell}(r)}{k^{2\ell+1}} + \mathscr{S}_{k,\ell}(r)\right)$$

- potential has delta-function (contact) term

$$V \supset u\delta^3(\vec{x})$$

- kinetic term of singular solution has contact term at the origin

$$\left(-\frac{\nabla^2}{2\mu}\right)\frac{1}{r} = \frac{4\pi}{2\mu}\delta^3(\vec{x})$$

- cancellation between them leads to renormalization condition

$$p_\ell(k) - k^{2\ell+1}\frac{i\mathscr{K}_\ell(k)}{\mathscr{J}_\ell(k)} + \frac{d^{2\ell+1}}{dr^{2\ell+1}}\left[\frac{(kr)^\ell}{(2\ell)!!}r\mathscr{S}_{k,\ell}\right](0)$$

$$= p_\ell(k_0) - k_0^{2\ell+1}\frac{i\mathscr{K}_\ell(k_0)}{\mathscr{J}_\ell(k_0)} + \frac{d^{2\ell+1}}{dr^{2\ell+1}}\left[\frac{(k_0 r)^\ell}{(2\ell)!!}r\mathscr{S}_{k_0,\ell}\right](0)$$

- renormalization scale

Full scattering state

S-matrix

$$S_\ell(k) = \frac{\mathcal{J}_\ell(-k)}{\mathcal{J}_\ell(k)} \frac{p_\ell(k) - k^{2\ell+1}\dfrac{i\mathcal{K}_\ell(k)}{\mathcal{J}_\ell(k)} - k^{2\ell+1}\dfrac{i\mathcal{K}_\ell(-k)}{\mathcal{J}_\ell(-k)}}{p_\ell(k)}$$

- by considering large k, one can determine the renormalized constant by UV cross sections

$$\frac{4\pi}{|p_\ell(k)|^2} = \frac{\sigma^\ell_{\mathrm{sc},0}}{(2\ell+1)k^{4\ell}} \qquad \mathrm{Im}\frac{4\pi}{p_\ell(k)} \approx -\frac{\sigma^\ell_{\mathrm{ann},0}}{(2\ell+1)k^{2\ell-1}}$$

Unitarized Sommerfeld enhancement factor

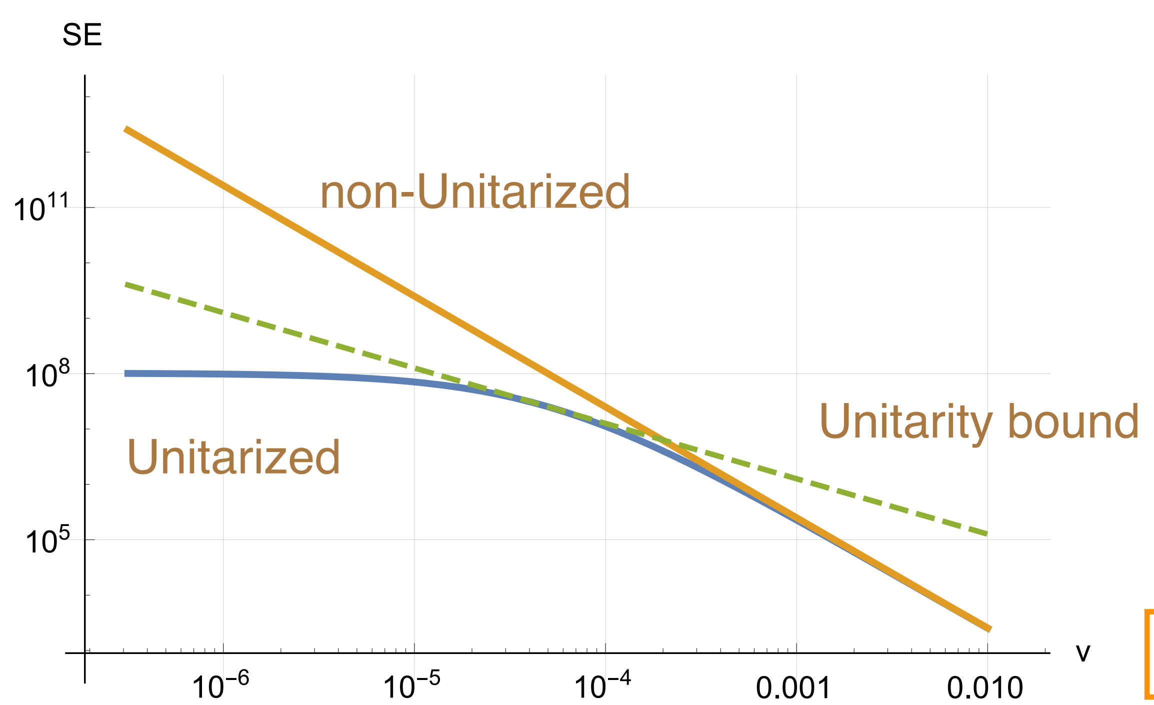

Blum, Sato and Slatyer, JHEP, 2016

Full scattering state

Bound state with decay width

AK, Matsumoto and Watanabe, in progress

- bound state is a pole of S-matrix
- non-Unitarized S-matrix has a pole at pure imaginary momentum

$$\mathcal{J}_\ell(k = i\kappa) = 0$$

- one can find the correction to the pole from Unitarized S-matrix by using properties of Jost function

$$\mathrm{Im}E_B = -\frac{1}{2(4\pi)}\frac{\sigma^\ell_{\mathrm{ann},0}v}{(2\ell+1)p^{2\ell}}\left|\frac{(2\ell+1)!!}{\ell!}\frac{d^\ell R^\ell_B}{dr^\ell}(0)\right|^2$$

$$\mathrm{Re}E_B = -\frac{\kappa^2}{2\mu}+\frac{1}{2(4\pi)\mu}\eta\sqrt{\frac{4\pi\sigma^\ell_{\mathrm{sc},0}}{(2\ell+1)p^{4\ell}}-\left(\frac{\sigma^\ell_{\mathrm{ann},0}}{(2\ell+1)p^{2\ell-1}}\right)^2}\left|\frac{(2\ell+1)!!}{\ell!}\frac{d^\ell R^\ell_B}{dr^\ell}(0)\right|^2$$

Data points

Overview

- cores in various-size halos

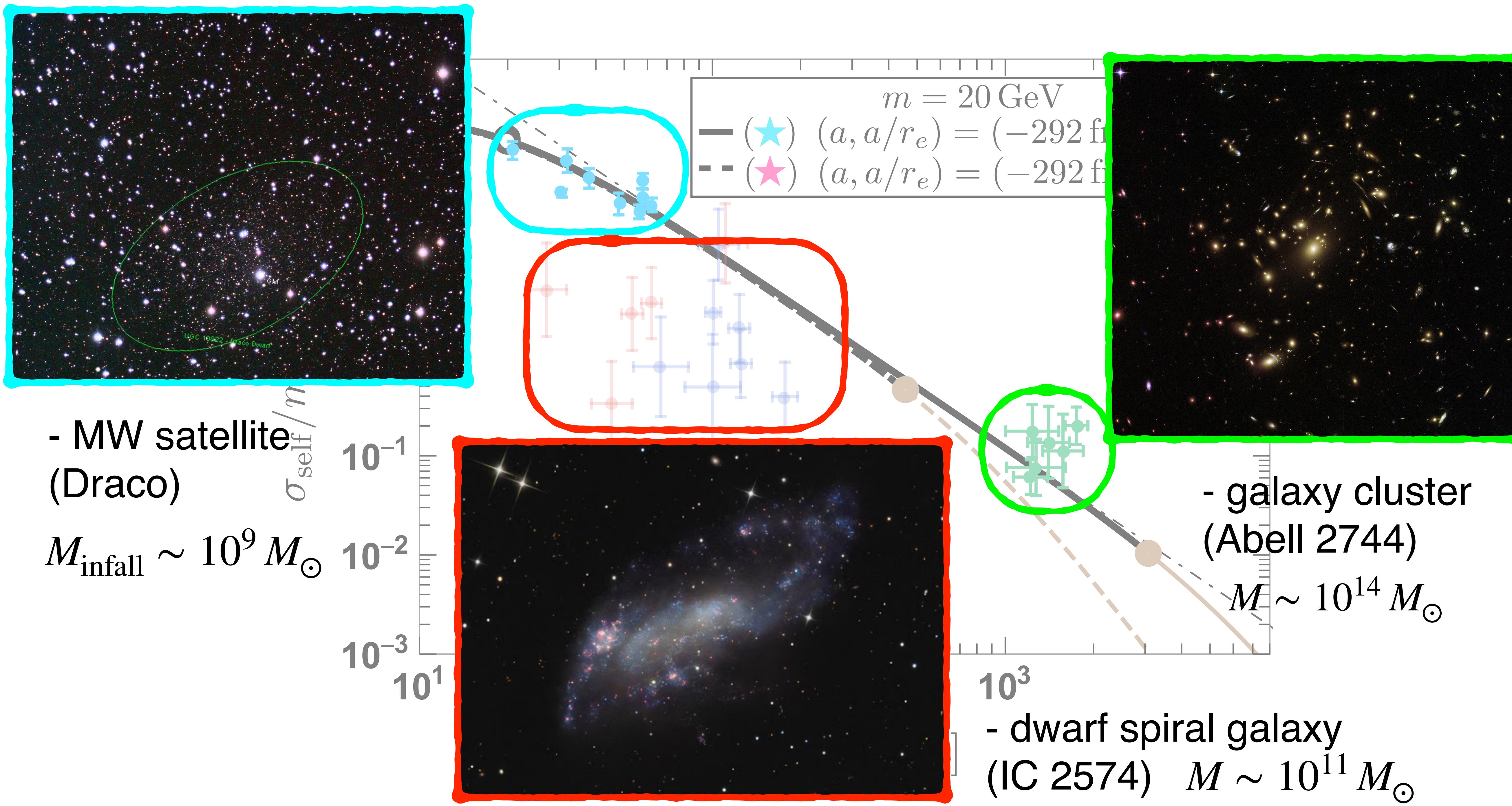

Data points

Galaxy clusters

- mass distribution in the outer region is determined by strong/weak gravitational lensing

- stellar kinematics in the central region (brightest cluster galaxies) prefer cored SIDM profile

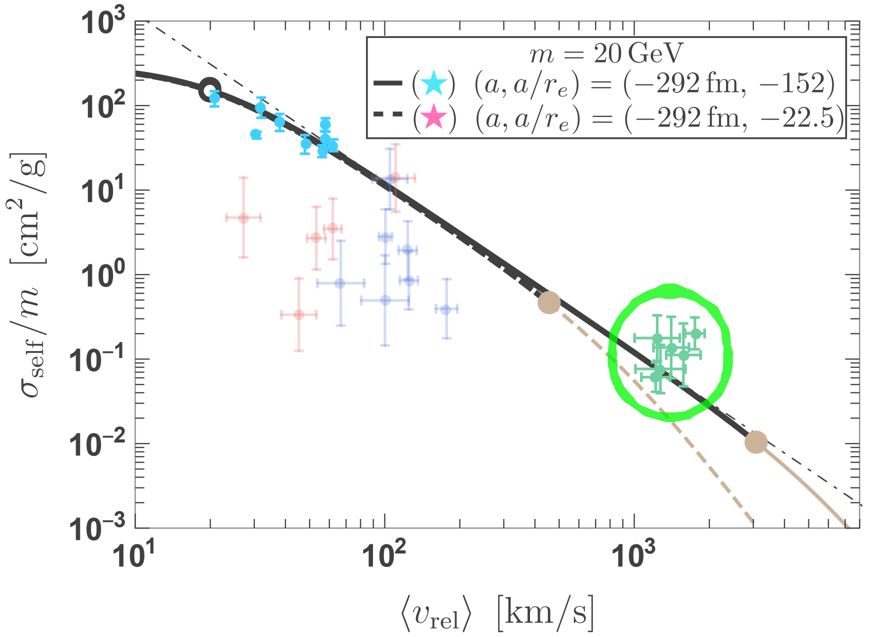

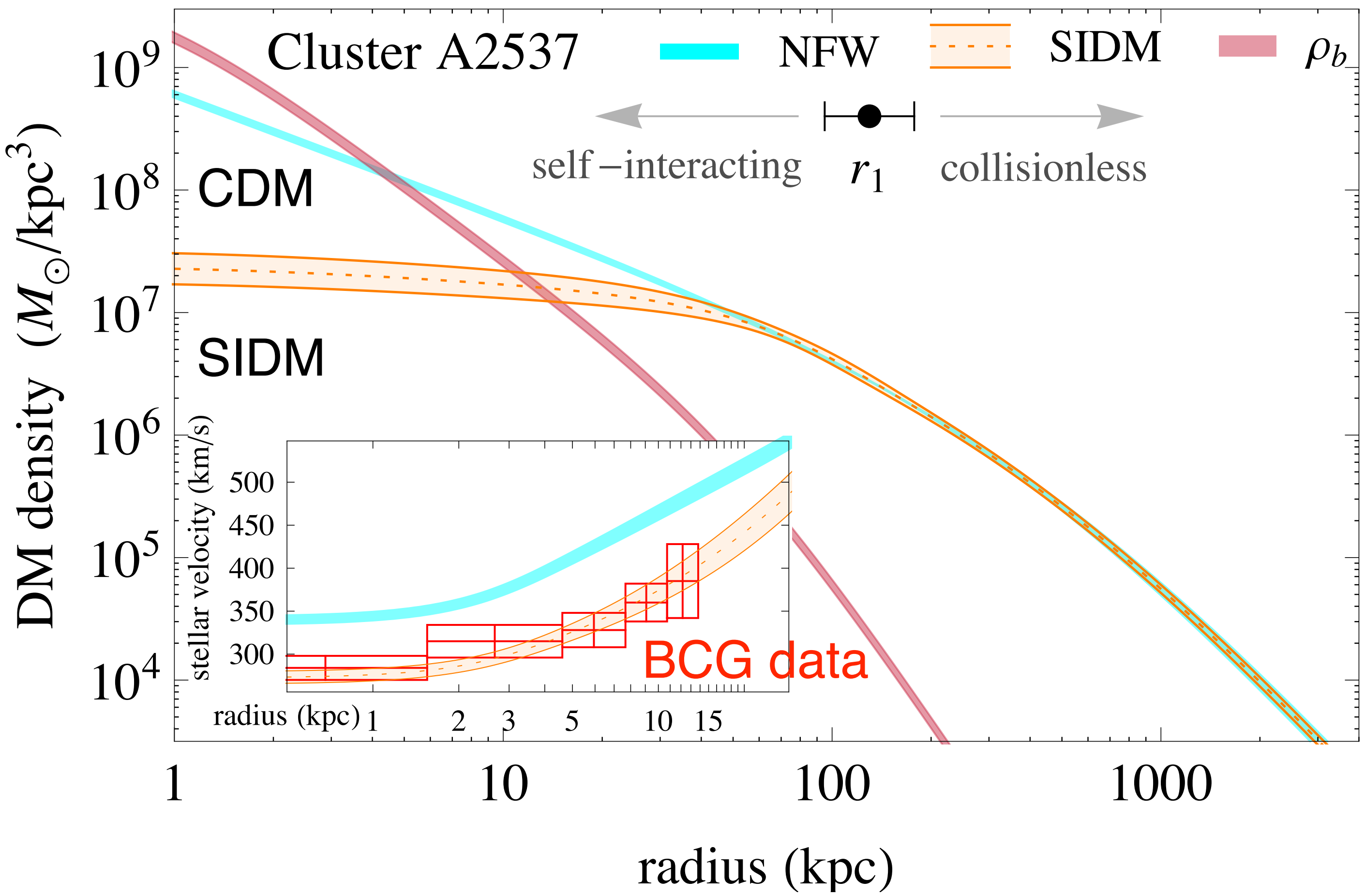

$$\sigma_{\rm self}/m \sim 0.1\,\mathrm{cm}^2/\mathrm{g}$$

$$\langle v_{\rm rel}\rangle \sim 10^3\,\mathrm{km/s}$$

Kaplinghat, Tulin and Yu, PRL, 2016

Data points

Dwarf spiral galaxies

- mass distribution is broadly determined by rotation curves

- rotation velocity in central region (of some galaxies) prefer cored SIDM profile

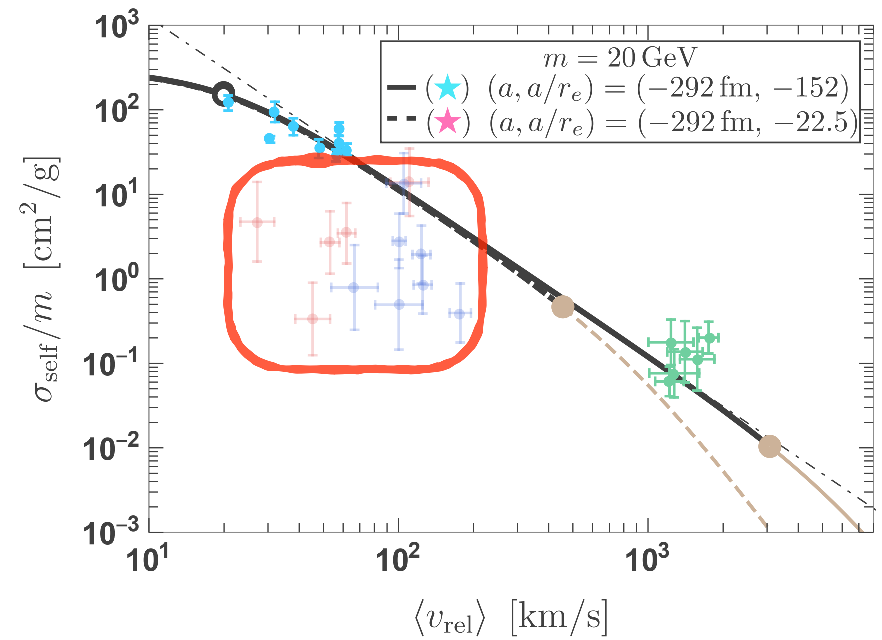

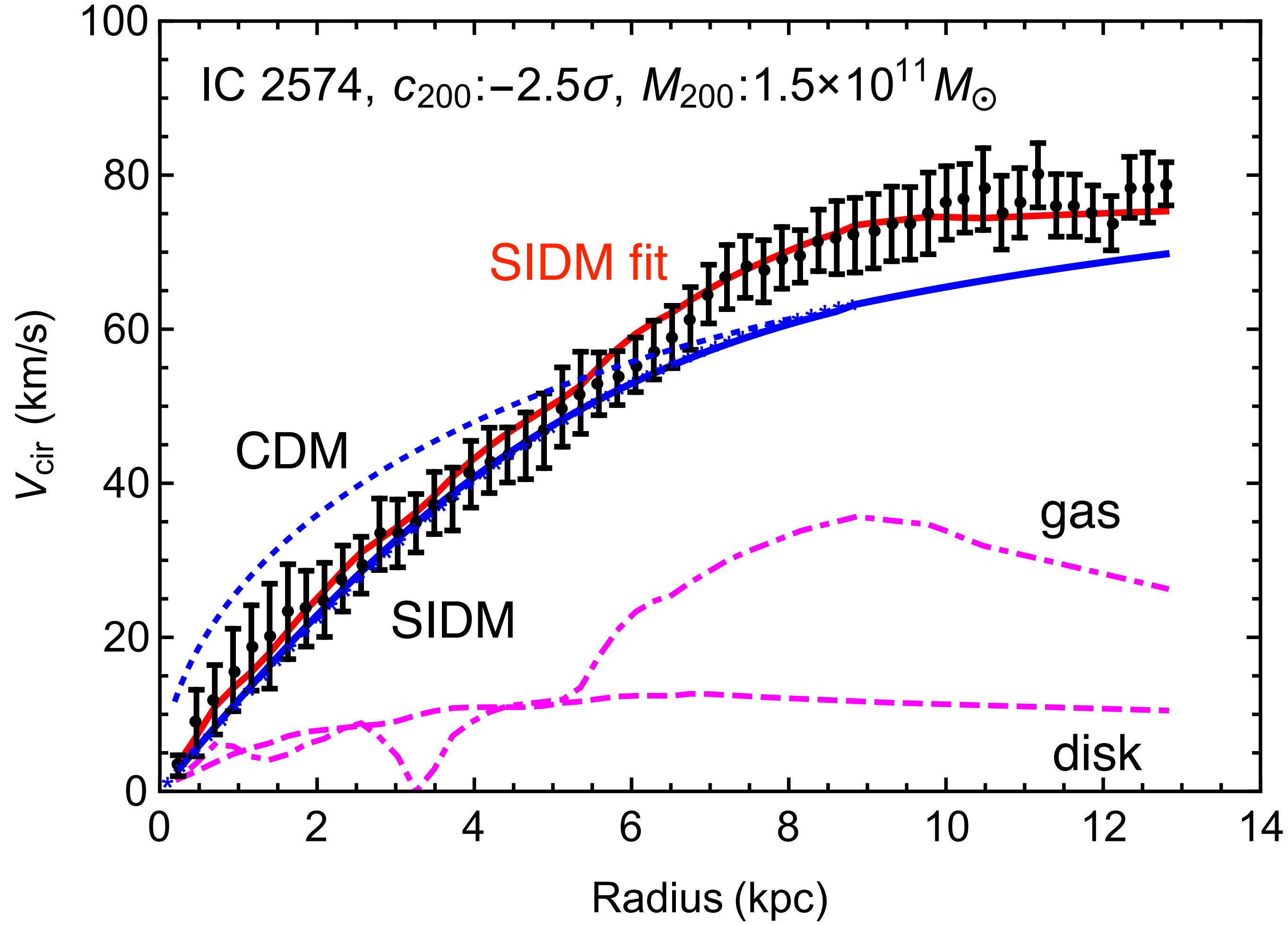

$$\sigma_\mathrm{self}/m \sim 1\,\mathrm{cm}^2/\mathrm{g}$$

$$\langle v_\mathrm{rel}\rangle \sim 10^2\,\mathrm{km/s}$$

AK, Kaplinghat, Pace and Yu, PRL, 2017

Data points

MW satellites

- mass distribution is determined by stellar kinematics

- stellar kinematics in the central region (of some satellites) prefer cuspy CDM profile

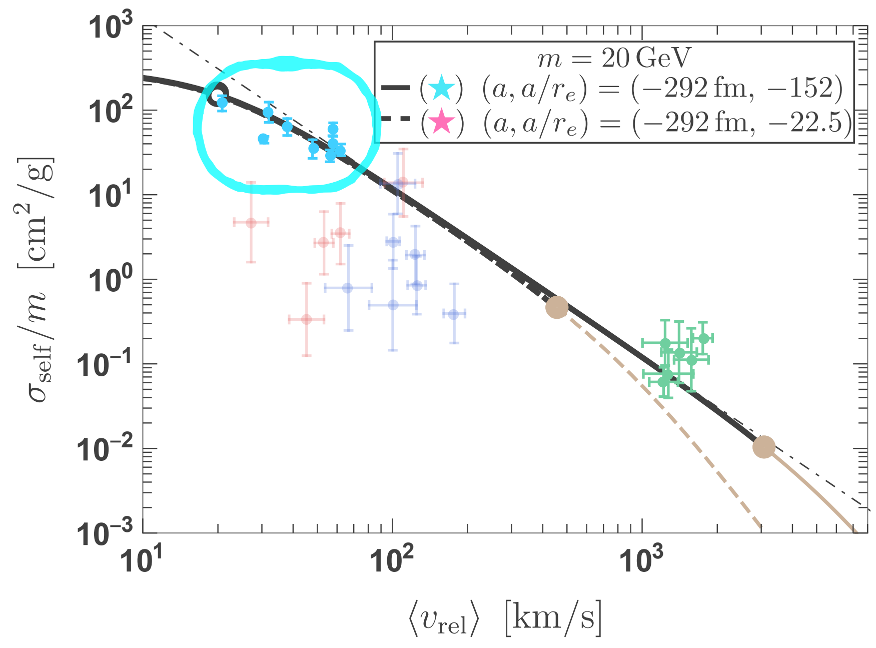

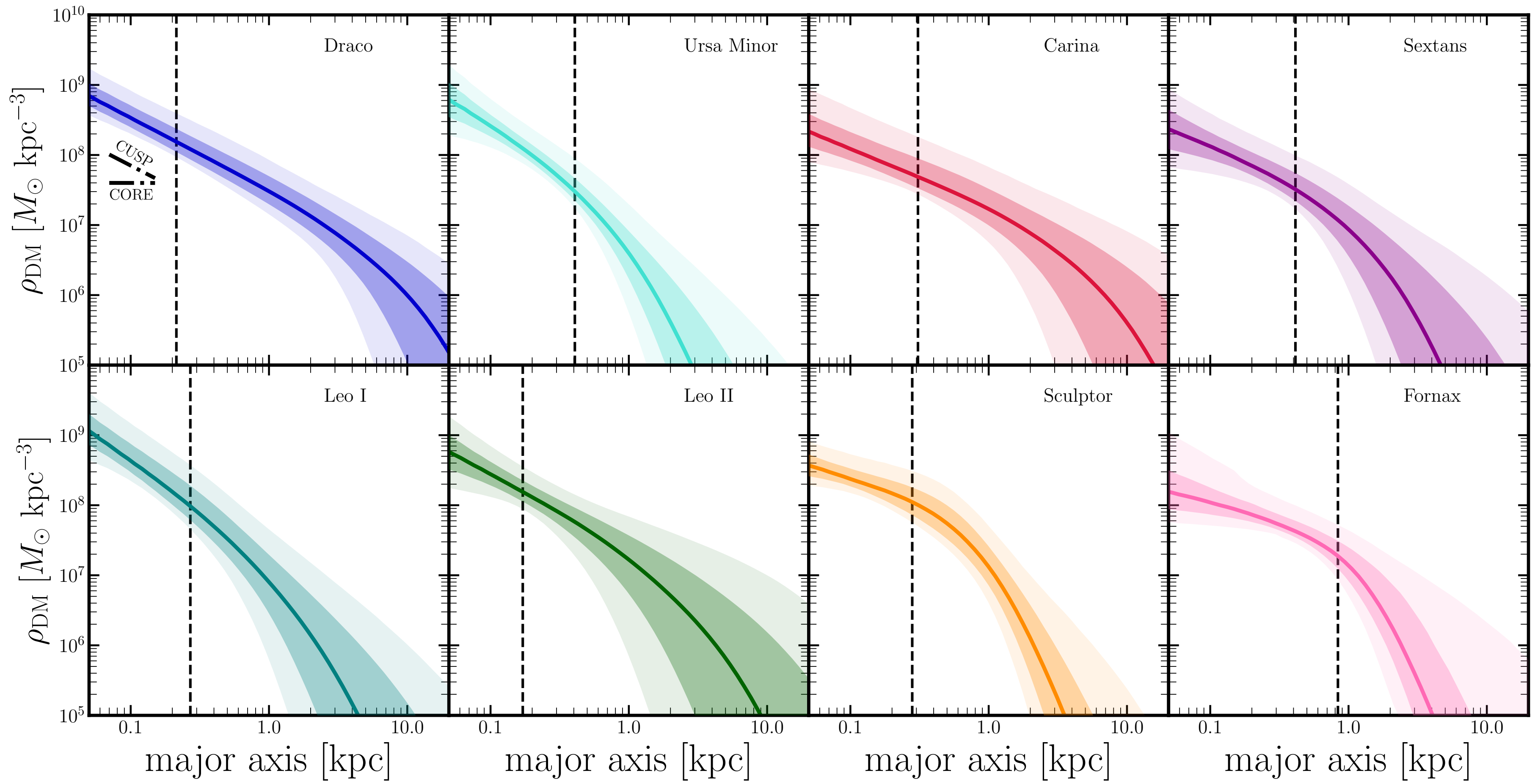

Hayashi, Chiba and Ishiyama, ApJ, 2020

Diversity in dwarf spiral galaxies

Rotation curves

- simulation: inner circular velocity is almost uniquely determined by outer circular velocity

$$\rho_{\mathrm{NFW}} = \frac{\rho_s}{r/r_s(1+r/r_s)^2}$$

- ρ_s and r_s are not independent (concentration-mass relation)

- observation: diverse inner circular velocity

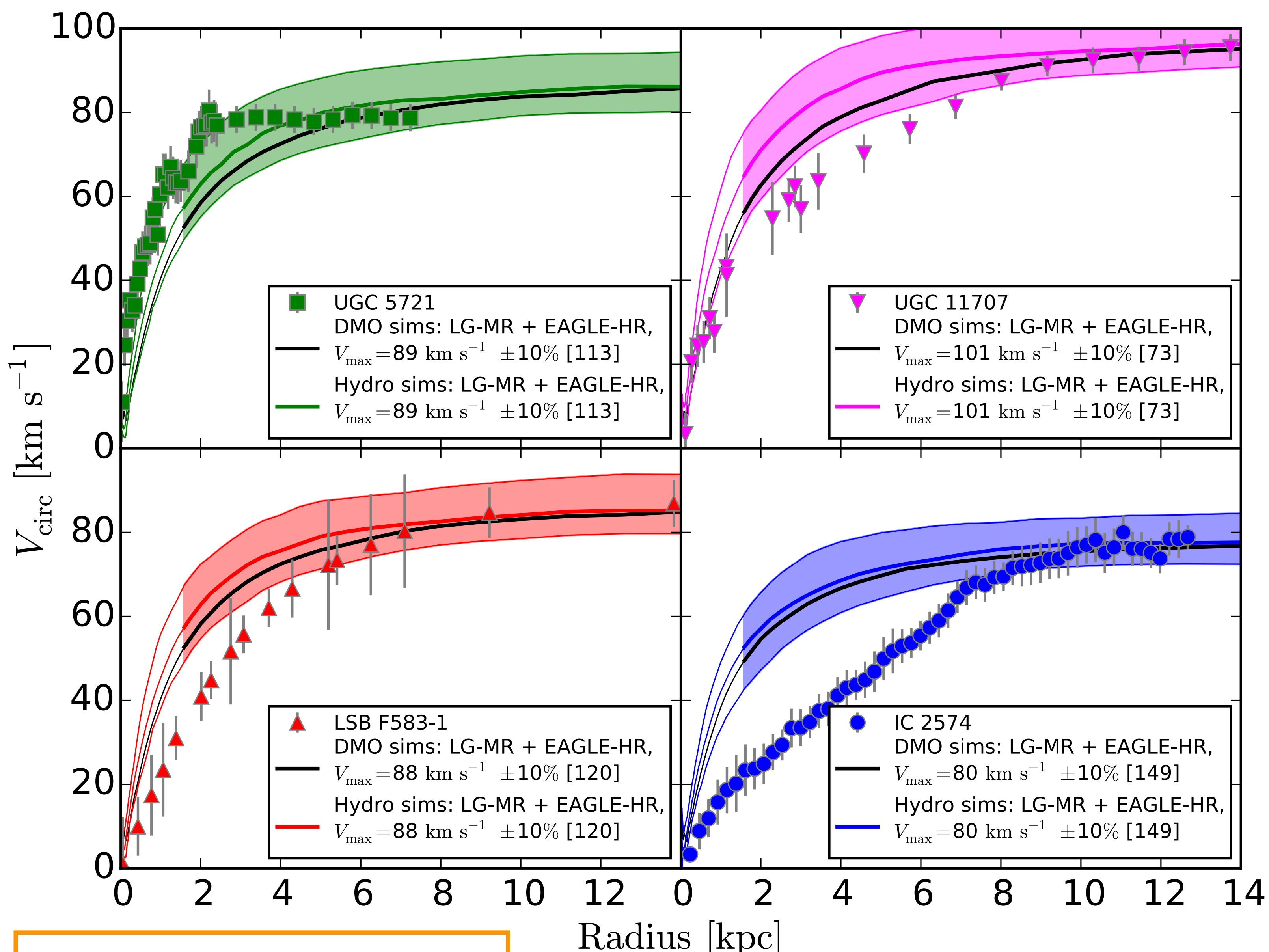

Oman *et al.*, MNRAS, 2015

Can SIDM explain it?

Naively, no

- SIDM has a universal impact

The unexpected diversity of dwarf galaxy rotation curves

Kyle A. Oman[1,⋆], Julio F. Navarro[1,2], Azadeh Fattahi[1], Carlos S. Frenk[3], Till Sawala[3], Simon D. M. White[4], Richard Bower[3], Robert A. Crain[5], Michelle Furlong[3], Matthieu Schaller[3], Joop Schaye[6], Tom Theuns[3]
[1] *Department of Physics & Astronomy, University of Victoria, Victoria, BC, V8P 5C2, Canada*
[2] *Senior CIfAR Fellow*
[3] *Institute for Computational Cosmology, Department of Physics, University of Durham, South Road, Durham DH1 3LE, United Kingdom*
[4] *Max-Planck Institute for Astrophysics, Garching, Germany*
[5] *Astrophysics Research Institute, Liverpool John Moores University, IC2, Liverpool Science Park, 146 Brownlow Hill, Liverpool, L3 5RF, United Kingdom*
[6] *Leiden Observatory, Leiden University, PO Box 9513, NL-2300 RA Leiden, the Netherlands*

4.5 The challenge to alternative dark matter models

Finally, we note that the diversity of rotation curves illustrated in Fig. 5 disfavours solutions that rely on modifying the physical nature of the dark matter. Cores can indeed be produced if the dark matter is SIDM or WDM but, in this case, we would expect *all* galaxies to have cores and, in particular, galaxies of similar mass or velocity to have cores of similar size. This is in disagreement with rotation curve data and suggests that a mechanism unrelated to the nature of the dark matter must be invoked to explain the rotation curve shapes.

Really? But galactic disks show diversity

- different disk sizes in different halos
- SIDM profile is exponentially sensitive to baryon distribution

$$\rho_{\rm DM}(\vec{x}) = \rho^0_{\rm DM} \exp(-\phi(\vec{x})/\sigma^2)$$

$$\Delta\phi = 4\pi G(\rho_{\rm DM} + \rho_{\rm baryon})$$

- iso-thermal region forms through self-interaction

SIDM explanation

SIDM reproduces diversity (unlike a naive expectation)

- compact disk→ redistribute SIDM significantly
- extended disk→ unchange SIDM distribution

$\sigma/m = 3\,\mathrm{cm}^2/\mathrm{g}$

AK, Kaplinghat, Pace, and Yu, PRL, 2017

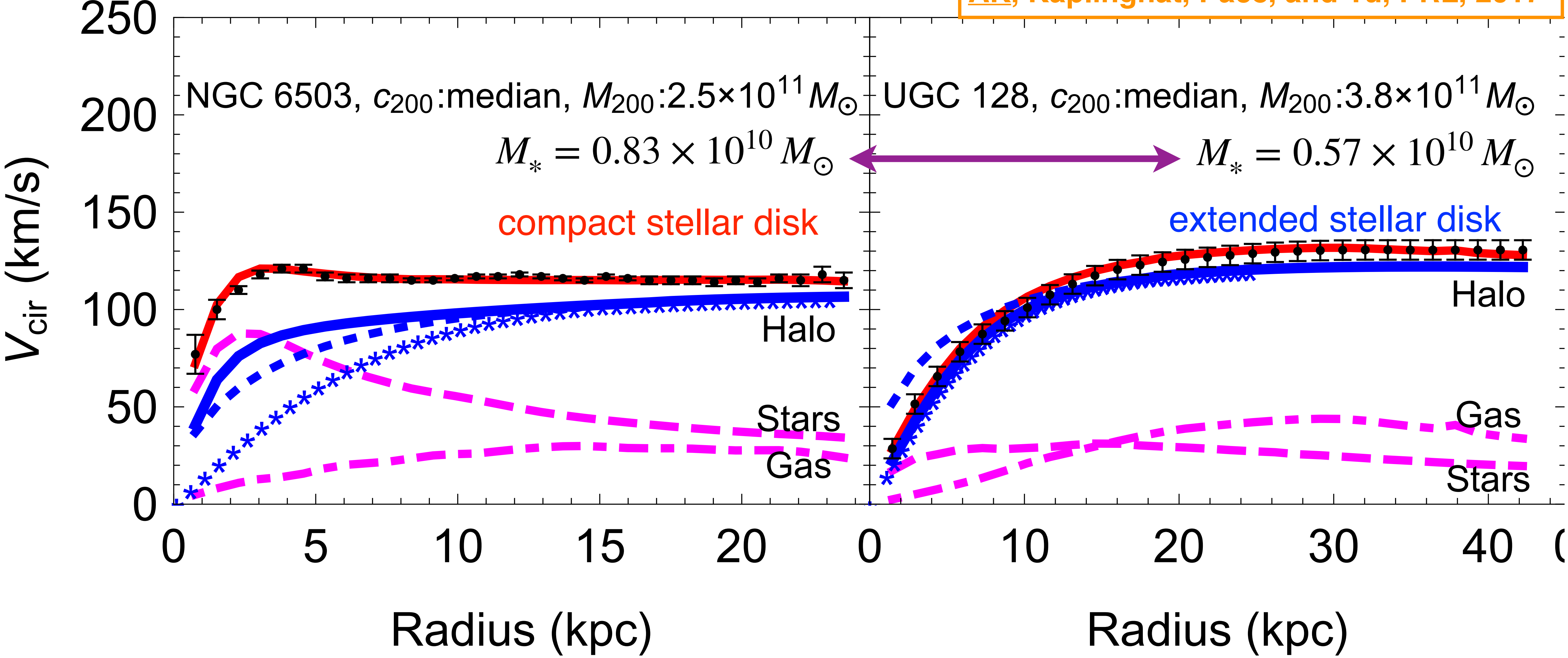

Diversity in MW satellites

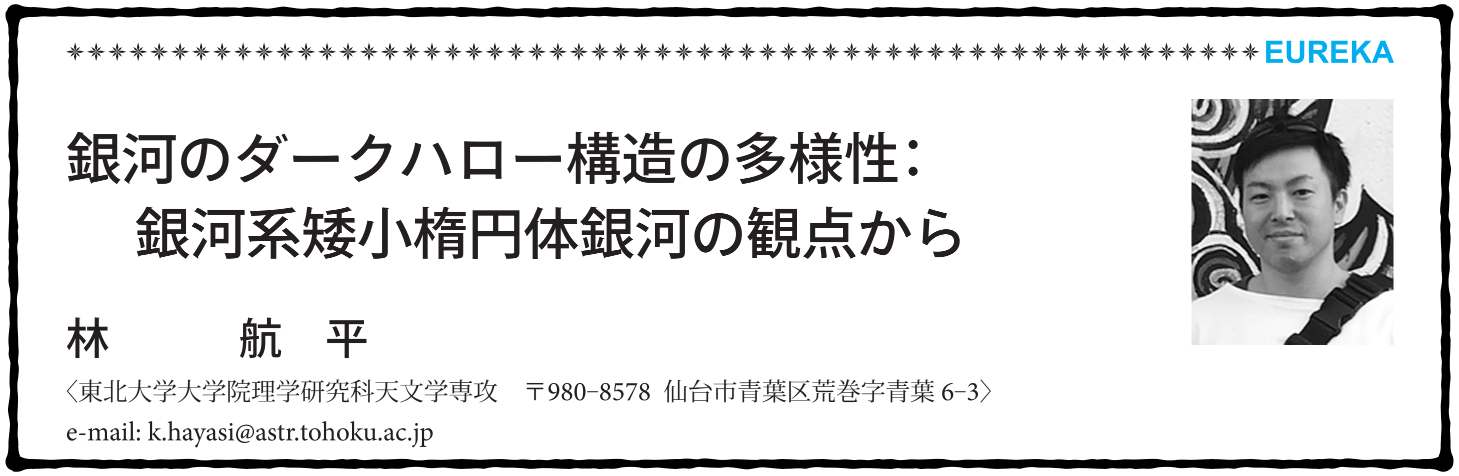
**EUREKA

銀河のダークハロー構造の多様性：
銀河系矮小楕円体銀河の観点から

林　　航平

〈東北大学大学院理学研究科天文学専攻　〒980-8578 仙台市青葉区荒巻字青葉 6-3〉
e-mail: k.hayasi@astr.tohoku.ac.jp

MW satellites (ultra-faint)

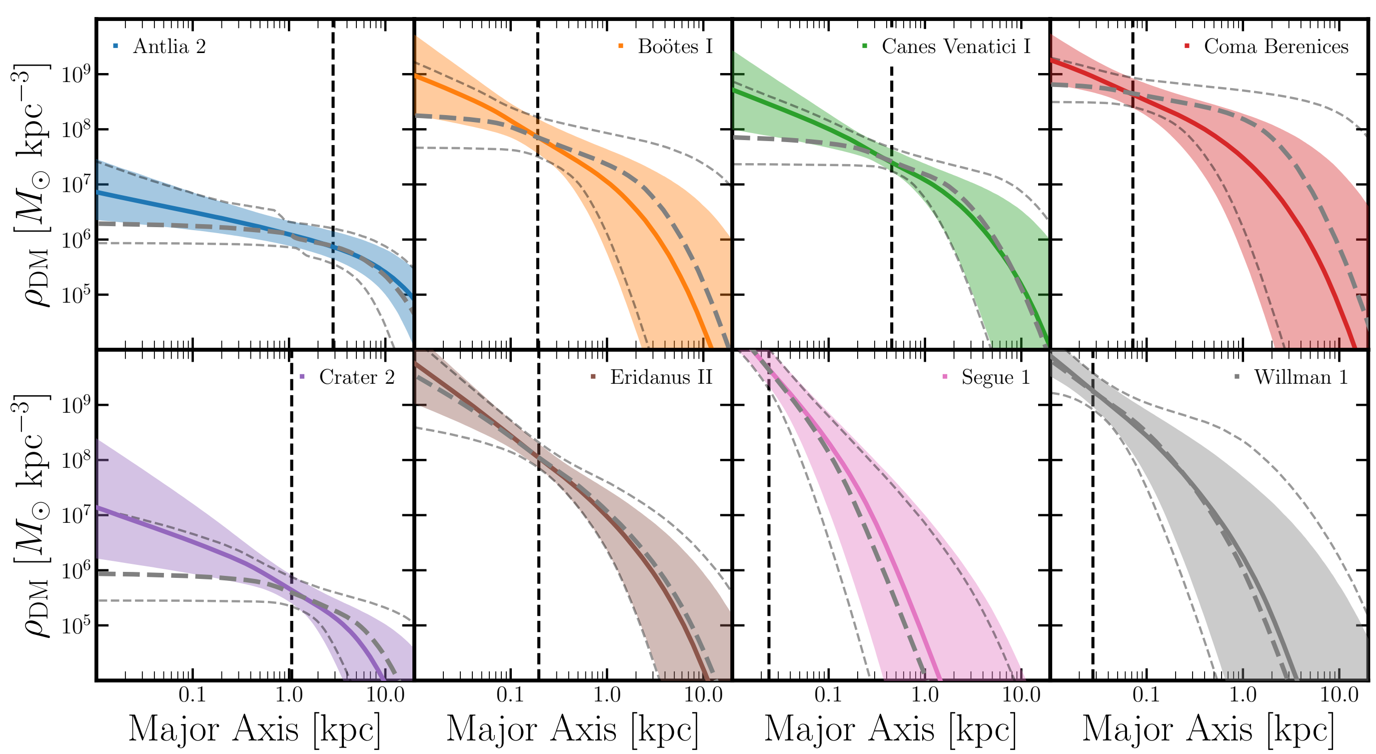

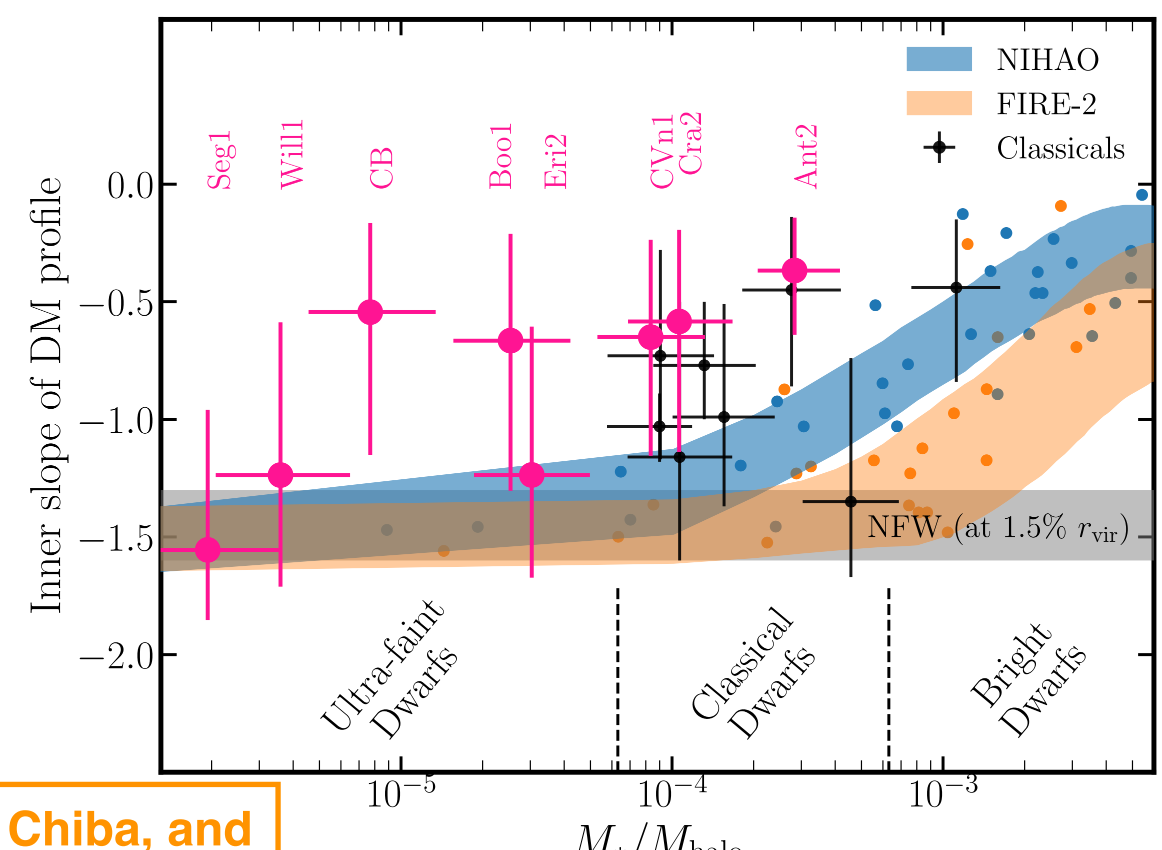

Hayashi, Hirai, Chiba, and Ishiyama, ApJ, 2023

SIDM halo evolution

Core formation

- core expansion lasts till the temperature profile gets flat (thermalization)

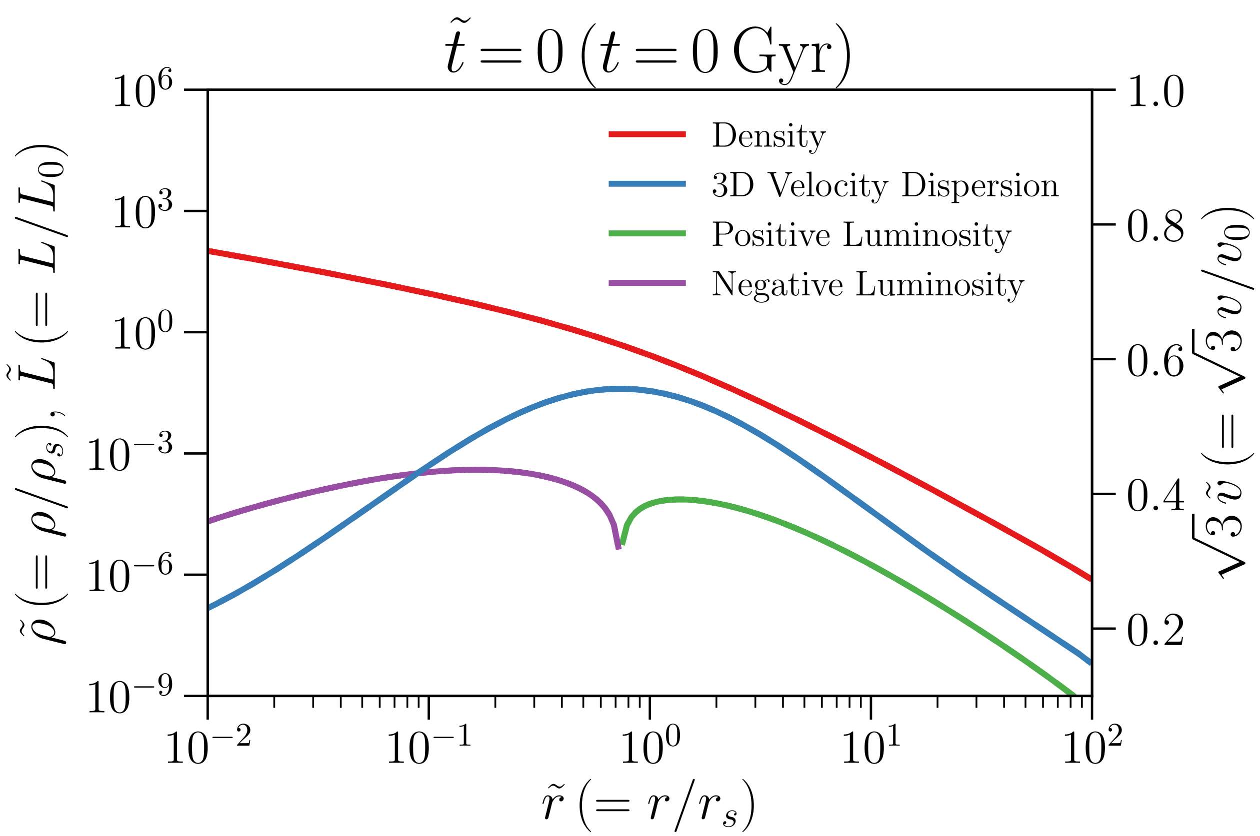

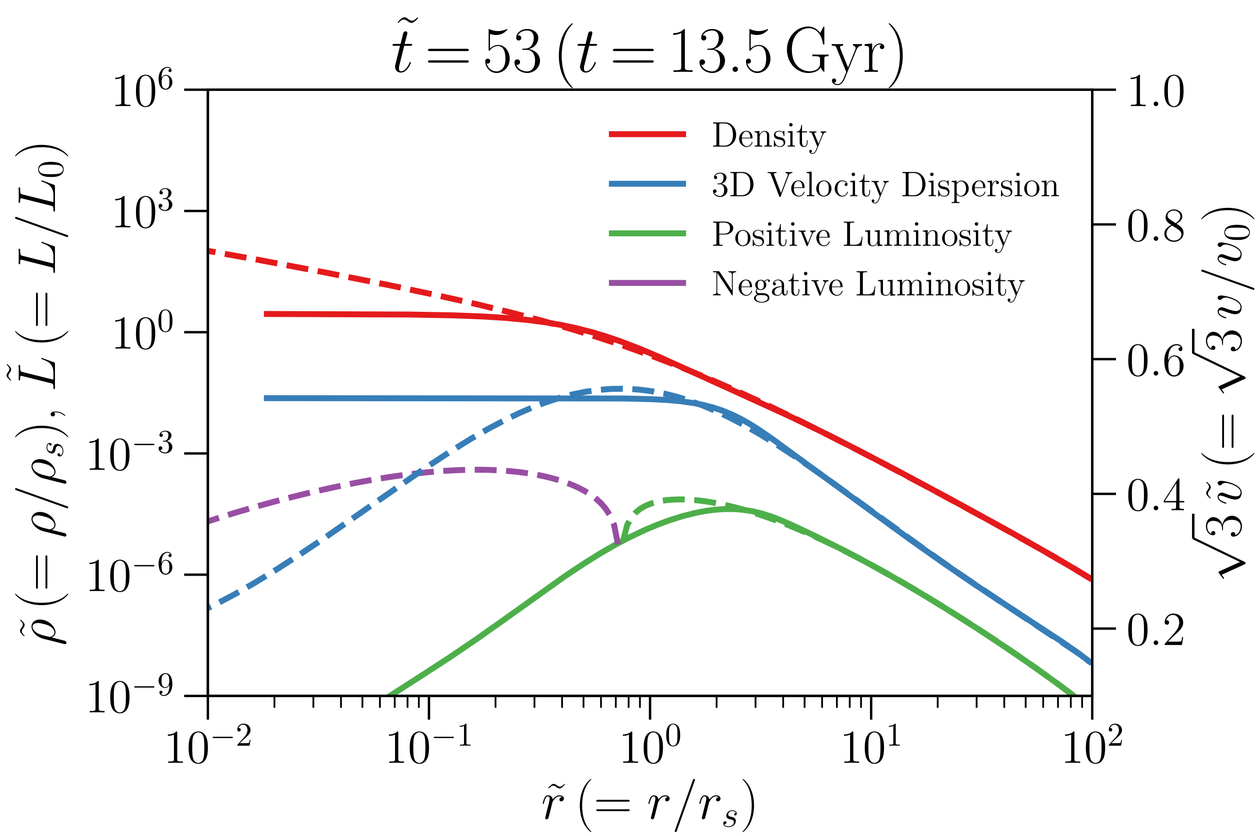

Nishikawa, Boddy, and Kaplinghat, PRD, 2020

SIDM halo evolution SIDM

Core collapse

- core collapse proceeds by depositing heat to the outer region

  - heat deposit → lower energy but higher temperature (negative heat capacity)

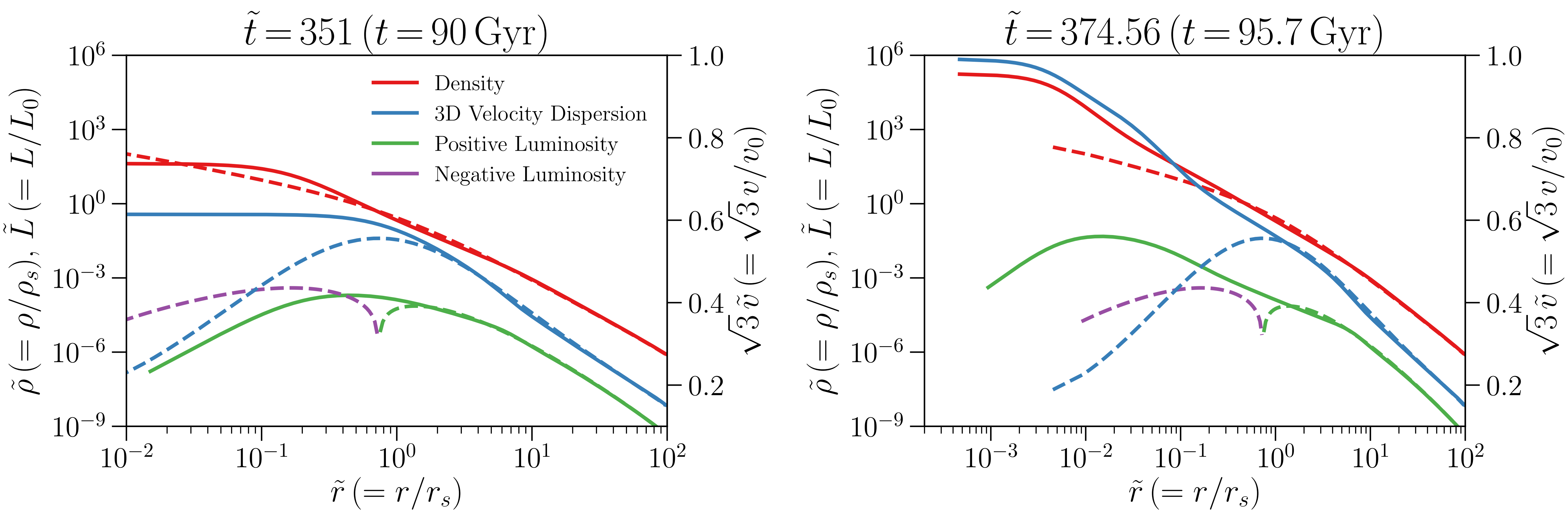

Nishikawa, Boddy, and Kaplinghat, PRD, 2020

On-going efforts

More precise prediction

- isolated halo + tidal stripping through gravothermal-fluid modeling
- cosmological simulations (time-consuming) are limited so far

How to examine?

- collapsed halos
    - through perturbations of strong-lensed systems

AN UNEXPECTED HIGH CONCENTRATION FOR THE DARK SUBSTRUCTURE IN THE GRAVITATIONAL LENS SDSSJ0946+1006

Quinn E. Minor
Department of Science, Borough of Manhattan Community College, City University of New York, New York, NY 10007, USA and Department of Astrophysics, American Museum of Natural History, New York, NY 10024, USA

Sophia Gad-Nasr and Manoj Kaplinghat
Department of Physics and Astronomy, University of California, Irvine CA 92697, USA

Simona Vegetti
Max Planck Institute for Astrophysics, Karl-Schwarzschild-Strasse 1, D-85740 Garching, Germany

Draft version November 24, 2020

ABSTRACT

The presence of an invisible substructure has previously been detected in the gravitational lens galaxy SDSSJ0946+1006 through its perturbation of the lensed images. Using flexible models for the main halo and the subhalo perturbation to fit the lensed images, we demonstrate that the subhalo has an extraordinarily high central density and steep density slope. The inferred concentration for

S and T matrices

Distorted-wave Born approximation

AK and Kuwahara, in progress

$$\mathcal{S}_{\text{brem}} = -2\pi i \delta(E - E' - \omega_k)\mathcal{T}_{\text{brem}}$$

$$\mathcal{T}_{\text{brem}} = \sum_n q_n e_\chi \, {}_{\text{out}}\langle \vec{P}', \vec{p}' | \left[e^{0*}(\vec{k}, \lambda) e^{-i\vec{k}\cdot\vec{x}_n} - \frac{1}{2m_n} \vec{e}^{\,*}(\vec{k}, \lambda) \cdot \left(e^{-i\vec{k}\cdot\vec{x}_n} \vec{p}_n + \vec{p}_n e^{-i\vec{k}\cdot\vec{x}_n} \right) \right] | \vec{p}, \vec{P} \rangle_{\text{in}}$$

- 2-body states (bra/ket) labeled by **asymptotic** (out/in) center-of-mass momentum and relative momentum

$$\vec{P} = \vec{p}_1 + \vec{p}_2 \qquad \vec{p} = \frac{1}{m_2}\vec{p}_2 - \frac{1}{m_1}\vec{p}_1 \qquad E = \frac{1}{2M}\vec{P}^2 + \frac{1}{2\mu}\vec{p}^2$$

$$= (2\pi)^3 \delta^3(\vec{P} - \vec{P}' - \vec{k}) \sum_n q_n e_\chi \left(e^{0*}(\vec{k}, \lambda) D_n^0 - \vec{e}^{\,*}(\vec{k}, \lambda) \cdot \vec{D}_n \right)$$

- momentum conservation

$$D_1^0 = {}_{\text{out}}\langle \vec{p}' | e^{i\frac{\mu}{m_1}\vec{k}\cdot\vec{r}} | \vec{p} \rangle_{\text{in}} \qquad \vec{D}_1 = \frac{1}{2M}(\vec{P}' + \vec{P}) D_1^0 - \frac{1}{2m_1} {}_{\text{out}}\langle \vec{p}' | \left(e^{i\frac{\mu}{m_1}\vec{k}\cdot\vec{r}} \vec{p} + \vec{p} e^{i\frac{\mu}{m_1}\vec{k}\cdot\vec{r}} \right) | \vec{p} \rangle_{\text{in}}$$

$$D_2^0 = {}_{\text{out}}\langle \vec{p}' | e^{-i\frac{\mu}{m_2}\vec{k}\cdot\vec{r}} | \vec{p} \rangle_{\text{in}} \qquad \vec{D}_2 = \frac{1}{2M}(\vec{P}' + \vec{P}) D_2^0 + \frac{1}{2m_2} {}_{\text{out}}\langle \vec{p}' | \left(e^{-i\frac{\mu}{m_2}\vec{k}\cdot\vec{r}} \vec{p} + \vec{p} e^{-i\frac{\mu}{m_2}\vec{k}\cdot\vec{r}} \right) | \vec{p} \rangle_{\text{in}}$$

$$\omega_k D_n^0 - \vec{k} \cdot \vec{D}_n = 0$$

- current conservation

S and T matrices

Dipole approximation

AK and Kuwahara, in progress

- good for non-relativistic scattering

$$\omega_k(\simeq \epsilon' - \epsilon), k = \mathcal{O}(v^2) \qquad \epsilon = \frac{1}{2\mu}\vec{p}^2$$

$$D_1^0 \simeq i\vec{k}\cdot\frac{\mu}{m_1}{}_{\rm out}\langle\vec{p}'|\vec{r}|\vec{p}\rangle_{\rm in} = i\frac{1}{m_1\omega_k^2}\vec{k}\cdot\overrightarrow{W} \qquad D_2^0 \simeq -i\frac{1}{m_2\omega_k^2}\vec{k}\cdot\overrightarrow{W}$$

- using commutation relations with $H_{0\chi}$

$$\overrightarrow{D}_1 \simeq \frac{1}{2M}(\overrightarrow{P}' + \overrightarrow{P})D_1^0 - \frac{1}{m_1}{}_{\rm out}\langle\vec{p}'|\vec{p}|\vec{p}\rangle_{\rm in} \simeq i\frac{1}{m_1\omega_k}\overrightarrow{W} \qquad \overrightarrow{D}_2 \simeq -i\frac{1}{m_2\omega_k}\overrightarrow{W}$$

$$\overrightarrow{W} = \langle\vec{p}'|\overrightarrow{\nabla}V(r)|\vec{p}\rangle = \int d^3r\psi^*_{{\rm out},\vec{p}'}(\vec{r})\left[\overrightarrow{\nabla}V(r)\right]\psi_{{\rm in},\vec{p}}(\vec{r})$$

$$\psi_{{\rm in},\vec{p}}(\vec{r}) \to e^{i\vec{p}\cdot\vec{r}} + f(\vec{p})\frac{e^{ipr}}{r} \qquad \psi_{{\rm out},\vec{p}}(\vec{r}) = \psi^*_{{\rm in},-\vec{p}}(\vec{r}) \to e^{i\vec{p}\cdot\vec{r}} + f(-\vec{p})^*\frac{e^{-ipr}}{r}$$